

**Peer Review** The peer review history for this article is available as a PDF in the Supporting Information.

**Key Points:**

- Carbonate saturation of the internal growth medium is reduced in modern Galápagos Porites corals, particularly following warm extremes
- Corals display similar capacity to regulate their growth medium among sites and time periods, with limited adaptation to acidification
- Taken together, these results suggest strict physiological limits to corals' ability to buffer against changing ocean conditions

**Supporting Information:**

Supporting Information may be found in the online version of this article.

**Correspondence to:**

D. Thompson,  
thompsond@arizona.edu

**Citation:**

Thompson, D., McCulloch, M., Cole, J. E., Reed, E. V., D'Olivo, J. P., Dyez, K., et al. (2022). Marginal reefs under stress: Physiological limits render Galápagos corals susceptible to ocean acidification and thermal stress. *AGU Advances*, 3, e2021AV000509. <https://doi.org/10.1029/2021AV000509>

Received 16 JUN 2021

Accepted 21 DEC 2021

**Author Contributions:**

**Conceptualization:** Diane Thompson, Malcolm McCulloch, Julia E. Cole, Alexander W. Tudhope  
**Data curation:** Diane Thompson, Malcolm McCulloch, Julia E. Cole, Emma V. Reed, Juan P. D'Olivo, Kelsey Dyez, Marcus Lofverstrom  
**Formal analysis:** Diane Thompson, Malcolm McCulloch, Julia E. Cole,

© 2022. The Authors.

This is an open access article under the terms of the [Creative Commons Attribution License](#), which permits use, distribution and reproduction in any medium, provided the original work is properly cited.

## Marginal Reefs Under Stress: Physiological Limits Render Galápagos Corals Susceptible to Ocean Acidification and Thermal Stress

Diane Thompson<sup>1</sup> , Malcolm McCulloch<sup>2</sup> , Julia E. Cole<sup>3</sup> , Emma V. Reed<sup>1</sup> , Juan P. D'Olivo<sup>4</sup>, Kelsey Dyez<sup>3</sup> , Marcus Lofverstrom<sup>1</sup> , Janice Lough<sup>5,6</sup> , Neal Cantin<sup>5</sup>, Alexander W. Tudhope<sup>7</sup>, Anson H. Cheung<sup>8</sup> , Lael Vetter<sup>1</sup> , and R. Lawrence Edwards<sup>9</sup> 

<sup>1</sup>University of Arizona, Department of Geosciences, Tucson, AZ, USA, <sup>2</sup>University of Western Australia, ARC Centre of Excellence for Coral Reefs Studies, Oceans Graduate School and Oceans Institute, Crawley, WA, Australia, <sup>3</sup>University of Michigan, Earth and Environmental Sciences, Ann Arbor, MI, USA, <sup>4</sup>Freie Universität Berlin, Berlin, Germany, <sup>5</sup>Australian Institute of Marine Science, Townsville, QLD, Australia, <sup>6</sup>ARC Centre of Excellence for Coral Reef Studies, James Cook University, Townsville, QLD, Australia, <sup>7</sup>University of Edinburgh, School of Geosciences, Edinburgh, UK, <sup>8</sup>Department of Earth, Environmental, and Planetary Sciences, Brown University, Providence, RI, USA, <sup>9</sup>Department of Earth Sciences, University of Minnesota, Minneapolis, MN, USA

**Abstract** Ocean acidification (OA) and thermal stress may undermine corals' ability to calcify and support diverse reef communities, particularly in marginal environments. Coral calcification depends on aragonite supersaturation ( $\Omega \gg 1$ ) of the calcifying fluid (cf) from which the skeleton precipitates. Corals actively upregulate  $\text{pH}_{\text{cf}}$  relative to seawater to buffer against changes in temperature and dissolved inorganic carbon, which together control  $\Omega_{\text{cf}}$ . Here we assess the buffering capacity of modern and fossil corals from the Galápagos Islands that have been exposed to sub-optimal conditions, extreme thermal stress, and OA. We demonstrate a significant decline in  $\text{pH}_{\text{cf}}$  and  $\Omega_{\text{cf}}$  since the pre-industrial era, trends which are exacerbated during extreme warm years. These results suggest that there are likely physiological limits to corals' pH buffering capacity, and that these constraints render marginal reefs particularly susceptible to OA.

**Plain Language Summary** Reef-building corals regulate their internal environment to permit rapid growth, which is critical for creating the structure and function of coral reefs. However, we demonstrate that there are finite limits to the ability of corals to regulate their internal chemistry to optimize growth. This limitation will leave corals susceptible to ocean warming and acidification, particularly in sub-optimal environments. Galápagos corals already display signs of stress and an inability to maintain an optimal internal growth environment from the eighteenth century to today.

### 1. Introduction

The carbonate structures of coral reef ecosystems provide critical defenses against storm surge and sea-level rise, supporting billions of dollars of goods and services annually beyond their intrinsic value (Spalding et al., 2017) and highlighting the need to understand how changing ocean conditions impact coral calcification. Thermal stress and ocean acidification (OA) diminish coral calcification, as shown in both experimental systems and Free Ocean  $\text{CO}_2$  Enrichment (FOCE) experiments on natural reefs (Gattuso et al., 2014). Analyses of coral density variations in cores of massive corals also reveal declining coral calcification through time (Lough, 2010). Collectively, these studies demonstrate spatially and temporally varying rates of calcification, with significant declines under recent extreme warming events and OA. Corals in the Galápagos Archipelago have been disproportionately impacted (Glynn et al., 2018), due to both extreme El Niño-related warming (Glynn, 2001; Glynn et al., 1988) and highly variable upwelling and pH/saturation state (Manzello, 2010; Manzello et al., 2008). These "marginal" reefs exhibit low species diversity and structural complexity (Cortés, 1997; Darwin & Bonney, 1889; Glynn, 2001; Glynn et al., 2017; Manzello et al., 2008), and have experienced acidification at rates of around  $-0.0026$  (pH units, total scale)  $\text{yr}^{-1}$  over the last 1.5 decades (1997–2011, Sutton et al., 2014). Differential recovery rates along spatial pH gradients (Manzello et al., 2014) further demonstrate the importance of carbonate chemistry and calcification processes to reef health in this region. As  $\text{CO}_2$  levels rise, changing patterns of OA and warming will increase the pressure on eastern equatorial Pacific and other marginal reef environments.

Emma V. Reed, Juan P. D'Olivo, Kelsey Dyez, Anson H. Cheung, Lael Vetter, R. Lawrence Edwards

**Funding acquisition:** Diane Thompson, Malcolm McCulloch, Julia E. Cole, Alexander W. Tudhope

**Investigation:** Diane Thompson

**Methodology:** Diane Thompson, Malcolm McCulloch, Janice Lough, Neal Cantin

**Project Administration:** Diane Thompson

**Resources:** Diane Thompson, Malcolm McCulloch, Julia E. Cole, Janice Lough, R. Lawrence Edwards

**Software:** Diane Thompson

**Supervision:** Diane Thompson

**Validation:** Diane Thompson

**Visualization:** Diane Thompson, Emma V. Reed

**Writing – original draft:** Diane Thompson

**Writing – review & editing:** Diane Thompson, Malcolm McCulloch, Julia E. Cole, Emma V. Reed, Juan P. D'Olivo, Kelsey Dyez, Marcus Lofverstrom, Janice Lough, Neal Cantin, Alexander W. Tudhope, Anson H. Cheung, Lael Vetter, R. Lawrence Edwards

A critical question remains, however: do corals have the adaptive capacity to maintain sustainable calcification in the face of increasingly stressful environmental conditions? Here, we leverage advances in biomineralization and boron isotope systematics to assess how changes in energy availability alter rates of calcification, the chemistry of the calcifying fluid, and the geochemistry of the carbonate skeleton (Table S1 in Supporting Information S1). We use this understanding of coral biomineralization to elucidate the susceptibility of coral calcification to OA and thermal stress, and to assess the adaptive capacity of Galápagos (*Porites* sp.) corals to changing ocean conditions.

In reef-building corals, calcification varies in response to internal (physiological) and external (environmental) factors, and maintenance of aragonite supersaturation in their calcifying fluid ( $\Omega_{\text{cf}} \gg 1$ ) is the ultimate factor that permits supercalcification and buffers against changes in seawater chemistry (McCulloch et al., 2012; Thompson, 2021). This state is achieved via upregulation of DIC and pH in response to changing environmental conditions. For example, during cooler seasons, corals upregulate the pH of their calcifying fluid ( $\text{pH}_{\text{cf}}$ ) in response to a drop in metabolic (i.e., from zooxanthellar photosynthesis and coral respiration) DIC, resulting from reduced temperature and light (e.g., D'Olivo & McCulloch, 2017; McCulloch et al., 2017; Ross et al., 2017, 2019). Cool temperatures also slow calcification kinetics and reduce the buffering capacity of the coral calcifying fluid (hereafter “thermodynamic” factors, Guo, 2019; Georgiou et al., 2015). By upregulating  $\text{pH}_{\text{cf}}$ , corals maintain a stable aragonite saturation state, shifting the carbonate reactions to favor carbonate ion during the winter months and preserving their ability to calcify despite large seasonal changes in DIC availability and temperature (as reviewed by Thompson, 2021). If these processes operate across species and reef environments, corals may be able to withstand changes in seawater pH ( $\text{pH}_{\text{sw}}$ ).

However, our understanding of coral biomineralization processes largely depends on studies of modern massive corals from regions with relatively low interannual climate and geochemical variability (Figures 1a and 1b). Although a few studies have leveraged natural  $\text{CO}_2$  seeps to study coral biomineralization under extreme conditions (Wall et al., 2016, 2019), corals likely respond differently to sharp spatial gradients compared to temporal variations. In many marginal reef environments, strong oceanographic variability and low aragonite saturation states make reef-building corals particularly susceptible to changing ocean conditions. Further, such marginal reefs provide a potential analogue of future reef patterns, as OA broadens the coverage of sub-optimal to marginal conditions.

Here, we capitalize on the large natural gradients across the Pacific in SST variability (Figure 1a) and aragonite saturation state (Figure 1b) to understand the range of coral responses to ongoing warming and acidification. We apply a multi-proxy, multi-site synthesis of coral geochemistry, backed by a novel Earth system modelling framework, to reconstruct and contextualize the impact of environmental stresses on calcification and resiliency in Galápagos corals. We leverage geochemical tracers of coral biomineralization (Table S1 in Supporting Information S1)—skeletal B/Ca ( $[\text{CO}_3^-]$ ),  $\delta^{11}\text{B}$  ( $\text{pH}_{\text{cf}}$ ), and U/Ca ( $[\text{CO}_3^-]$ )—that constrain the calcifying fluid chemistry, including the aragonite saturation that governs calcification rate (DeCarlo et al., 2015, 2018). We combine these with paleo-environmental tracers that primarily reflect factors external to the coral calcification environment (Table S1 in Supporting Information S1): Sr/Ca (Beck et al., 1992; Corrèe et al., 2000), Li/Mg (Hathorne, Felis, et al., 2013; Montagna et al., 2014), and  $\delta^{18}\text{O}$  (McConaughey, 1989; Weber & Woodhead, 1972; all primarily controlled by SST); Ba/Ca (upwelling, Lea et al., 1989; G. T. Shen et al., 1992); and  $\delta^{13}\text{C}$  (upwelling, metabolic carbon/photosynthesis, respiration, and reproduction, G. T. Shen et al., 1992). These new recent (1976–2010) and fossil (1729–1733) Galápagos records (Wolf Island,  $1^\circ 23.15'\text{N}$ ,  $91^\circ 49.90'\text{W}$ ) significantly extend the multi-tracer data coverage prior to the industrial era, which allows us to assess the capacity of corals to buffer against changing environmental conditions. We compare our new Galápagos results with published data from the Great Barrier Reef (M. T. McCulloch et al., 2017) to contextualize results from the marginal Galápagos reef environment—a comparatively cold, low-saturation, and highly variable environment. Finally, we establish a comprehensive spatiotemporal framework for these results using simulations of ocean biogeochemistry that extend from pre-industrial to modern (Figure 1c), permitting the first cross-Pacific, multi-century synthesis of corals' ability to buffer calcifying fluid chemistry in response to changing ocean conditions, including acidification, warming, and (internal and forced) climate variability.

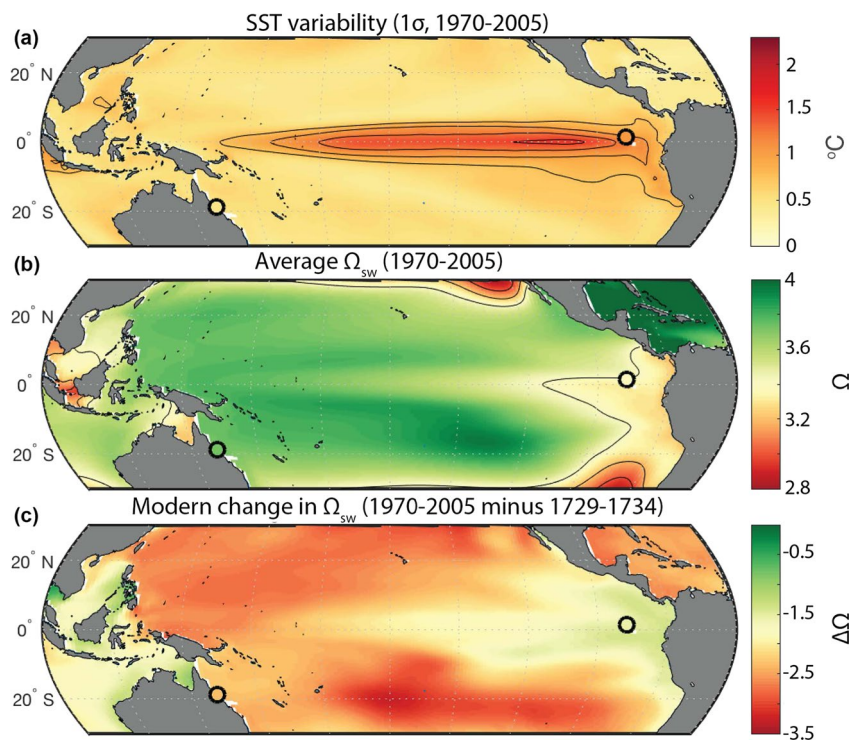


**Figure 1.** Map of study sites across tropical Pacific Ocean: (a) Interannual variability in sea-surface temperature (SST), calculated from standard deviation of CESM1 LME SST (see Figure S2 in Supporting Information S1 for validation against IGOSS SSTs, Reynolds et al., 2002); (b) aragonite saturation state  $\Omega_{sw}$  at 0 m, calculated using CO2SYS (Lewis et al., 1998) from CESM1 LME temperature, salinity,  $pH_{sw}$ , and seawater dissolved inorganic carbon (DIC<sub>sw</sub>) over the climatological period (1970–2005); and (c) difference in CESM1 LME  $\Omega_{sw}$  between the modern and eighteenth century periods studied here. Simulated values for the Great Barrier Reef (Davies Reef) and Galápagos (Wolf Island) study sites are indicated by filled circles; validation of CESM1 against observational values can be found in Table S3 in Supporting Information S1.

## 2. Data and Methods

### 2.1. Coral Core Collection

We collected cores from modern (living) and underwater sub-fossil (i.e., deceased upon collection; hereafter “fossil”) *Porites lobata* colonies in Shark Bay, along the northeastern shore of Wolf Island, Galápagos (1°23.15'N, 91°49.90'W) in May–June 2010. Here, we analyze four cores from three colonies (two modern, and one fossil): (a) GW10-3 (modern), collected from 10 m depth; (b) GW10-10 (modern), collected from 12 m depth; and (c) GW10-4 and (d) GW10-5 collected from the same fossil colony at 13 m depth. We compare these geochemical records from Wolf to published data from Davies Reef, Great Barrier Reef (cores 13–2 and 13–3, M. T. McCulloch et al., 2017).

### 2.2. Sub-Sampling & Age Determination

All cores were milled for geochemical analysis at continuous 2 mm increments in 5 mm-wide transects along the maximum growth axis; based on average modern extension rates (GW10-3 = 12.4 mm/year, GW10-10 = 20.3 mm/year), this sampling increment resolves sub-seasonal (bimonthly or better) variability of coral skeletal geochemistry and inferred environmental parameters. This resolution was selected based on the time- and sample-intensive nature of the ion exchange chromatography required for boron isotopic analysis; this work significantly extends the network of long, high-resolution, multi-proxy data. Modern corals were re-sampled adjacent to the original sampling transects (Jimenez et al., 2018) across intervals of known climatic extremes (e.g., large eastern Pacific El Niño events) and phases of Pacific decadal variability, while fossil cores were sampled prior to and following the depths sampled for U/Th age dating (to maximize precision of replicating and splicing these floating chronologies).

Pre-industrial Wolf fossil cores (WLF10-04 and WLF10-5) were U/Th dated at the University of Minnesota following the procedures of (Cheng et al., 2013; Edwards et al., 1987; C. C. Shen et al., 2002). Wolf10-04 and WLF10-05 sample ages were  $1732 \pm 7$  and  $1738 \pm 5$  C.E., respectively (see Reed et al., 2021 for full U/Th results). These floating chronologies were tied to the complete Sr/Ca record from WLF10-4 (Reed et al., 2021) to optimize correlation among the series within the uncertainty of the U/Th dates. However, all Wolf fossil coral series are floating chronologies (i.e., they are not tied to overlapping modern records); thus, we estimate an absolute age error as  $\pm 5$ –7 years (based on the precision of the U/Th dates).

Age-depth models for all cores were developed using linear interpolation in MATLAB between seasonal Sr/Ca-SST tie points. Due to high interannual variability in the timing of the cool season minima, the age model relies only on warm-season tie points. Sr/Ca minima were tied to March SST maxima; tie points for modern Wolf cores (WLF10-3 and WLF10-10) are identical to those published in Jimenez et al. (2018). Data were linearly interpolated to obtain monthly records for time-series analysis. Although this approach may introduce sub-annual chronological errors, regressions among geochemical proxies that form the core of this study were performed on the raw data (prior to age modeling) and are not influenced by chronological errors or interpolation. Finally, we used Sr/Ca-SST reconstructions from GW10-3 (2010–1987; 1983–1940) and GW10-10 (2010–1985; 1982–1975) published by Jimenez et al. (2018) and Cheung et al. (2021) for comparison.

### 2.3. Trace Elemental Geochemistry

All trace elemental analyses were performed on a Quadrupole-ICP-MS (X-series II Q-ICP-MS, Thermo Fisher Scientific) at the University of Western Australia. First, sub-samples of  $10 \pm 0.2$  mg of coral powder were weighed, dissolved in 500  $\mu$ L of 0.51N HNO<sub>3</sub>, agitated, and centrifuged for 1 min at 3500 rpm. A 38  $\mu$ L aliquot of dissolved powder was diluted in 3 mL of 2% HNO<sub>3</sub> (100 ppm Ca) for trace elemental analysis; the remaining 400  $\mu$ L of the dissolved powder was used for boron isotope analysis (see below). Analysis of <sup>7</sup>Li, <sup>25</sup>Mg, and <sup>11</sup>B by Q-ICP-MS was performed on the 100 ppm Ca dilution, while an additional 300  $\mu$ L sub-aliquot of the 100 ppm Ca solution was diluted (to 10 ppm Ca) in 2.7 mL of a 2% HNO<sub>3</sub> spike solution (containing  $\sim 19$  ppb <sup>45</sup>Sc, 19 ppb <sup>89</sup>Y, 0.19 ppb <sup>141</sup>Pr, and 0.095 ppb <sup>209</sup>Bi) for analysis of <sup>25</sup>Mg, <sup>43</sup>Ca, <sup>86</sup>Sr, and <sup>238</sup>U. Although some recent work suggests that organic matter may bias TE/Ca values and increase analytical uncertainty (particularly for Li/Mg, Cuny-Guirriec et al., 2019), these issues were reported for green, organic-rich bands in the skeleton. As there were no green, organic-rich bands in these cores, we did not pre-treat the samples prior to geochemical analysis to avoid offsets and noise that can arise from oxidative cleaning under certain conditions (Holcomb et al., 2015; Sayani et al., 2021). Nevertheless, we note that the presence of organic matter in the samples could have caused small (1%–4%) variations in trace elemental ratios and add noise to our data. Reproducibility for the JCP-1 interlaboratory standard ( $2\sigma$  relative standard deviation, RSD;  $n = 19$ ) was  $\pm 0.830\%$  for Mg/Ca,  $\pm 0.636\%$  for Sr/Ca,  $\pm 1.341\%$  for U/Ca,  $\pm 3.649\%$  for Li/Mg ( $N = 17$ ), and  $\pm 3.651\%$  for B/Mg ( $N = 17$ ). The long-term laboratory values for JCp-1 are well within the robust standard deviation of reported values from Hathorne, Gagnon, et al. (2013): Mg/Ca  $4.211 \pm 0.024$  mmol/mol ( $n = 173$ ), Sr/Ca  $8.848 \pm 0.0194$  mmol/mol ( $n = 173$ ), Ba/Ca  $7.297 \pm 0.242$   $\mu$ mol/mol ( $n = 159$ ), U/Ca  $1.194 \pm 0.0092$   $\mu$ mol/mol ( $n = 165$ ), Li/Mg  $1.441 \pm 0.0325$  mmol/mol ( $n = 144$ ), and B/Ca  $458.956 \pm 11.790$   $\mu$ mol/mol ( $n = 144$ ; see also D'Olivo et al., 2018).

We used published TE/Ca-SST calibrations to reconstruct SST from the (local) Sr/Ca-SST (M. T. McCulloch et al., 2017; Jimenez et al., 2018) and Li/Mg-SST (Montagna et al., 2014) relationships. For Wolf corals, we applied the Sr/Ca-SST calibration:

$$Sr/Ca_{coral}(\text{mmol/mol}) = -0.057(\pm 0.001) \times SST + 10.658(\pm 0.025) \quad (1)$$

From weighted least squares regression of the WLF10-03 and WLF10-10 composite record against OISST between May 1987–March 2010 (Jimenez et al., 2018). The composite calibration was utilized to standardize the calibrations across cores; however, the same results were found when using core-specific calibrations for the modern corals, as the calibration equations were similar between cores (Jimenez et al., 2018). For the Davies Reef, GBR corals, we used the Sr/Ca-SST calibration obtained from local calibration with in-situ temperature data (M. T. McCulloch et al., 2017):

$$Sr/Ca_{coral}(\text{mmol/mol}) = -0.046 \times SST + 10.12. \quad (2)$$

For both sites, the Li/Mg-SSTs were calculated using the calibration curve of Montagna et al. (2014). All new trace elemental geochemical data are shown in Figure 4 and S9–S10 in Supporting Information S1.

#### 2.4. Determination of Calcifying Fluid pH and Carbonate Chemistry From Boron Systematics

The boron in the remaining 400  $\mu\text{L}$  aliquot of dissolved powder (after trace elemental analysis, above) was purified by ion exchange chromatography (after M. T. McCulloch et al., 2014), and the  $\delta^{11}\text{B}$  was measured by MC-ICP-MS using a NU Plasma II at the University of Western Australia. The measured isotopic ratio of  $^{11}\text{B}$  and  $^{10}\text{B}$  of the carbonate samples were expressed relative to that of the NIST SRM 951 boric acid standard, in standard delta notation (in units of per mil or ‰):

$$\delta^{11}\text{B}_{\text{carb}} = \left[ \frac{^{11}\text{B}/^{10}\text{B}}{^{11}\text{B}/^{10}\text{B}_{\text{standard}}} \right] \times 1000. \quad (3)$$

Reproducibility for the JCP-1 interlaboratory standard across these runs ( $2\sigma; n = 29$ ) was  $\pm 0.22\text{\textperthousand}$ . Further, the long-term laboratory JCP-1 value and reproducibility of  $24.36 \pm 0.34\text{\textperthousand}$  ( $2\sigma; n = 101$ ; see also D’Olivo & McCulloch, 2017) agree well with reported values with and without oxidative pre-treatment (Gutjahr et al., 2021). Therefore, although the analytical uncertainty of our results may be slightly higher because the samples were not pre-cleaned (Gutjahr et al., 2021), the reported values are well within error of the pre-cleaned values from Gutjahr et al. (2021). The  $2\sigma$  uncertainties in this study are on par with that of pre-cleaned samples ( $n = 29$ ), while the long-term average falls between that of published values with and without cleaning ( $n = 101$ ). Finally, previous work suggests that  $\delta^{11}\text{B}$  is relatively insensitive to sample cleaning methods (Holcomb et al., 2015).

We used paired boron isotope and B/Ca ratios to determine the pH and carbonate ion concentration, leveraging three key features of boron isotope systematics (as reviewed by DeCarlo et al., 2018; Thompson, 2021). First, boron speciation in seawater depends strongly on pH, with borate ion ( $\text{B}(\text{OH})_4^-$ ) dominating at higher pH and boric acid ( $\text{B}(\text{OH})_3$ ) dominating at lower pH ( $<\sim 8.5$ ). Second, boron isotopes are strongly fractionated between the two species, with a  $+27\text{\textperthousand}$  offset between borate and boric acid. Taken together, as pH decreases, the fraction of boron as borate decreases and the  $\delta^{11}\text{B}$  increases. Third, as corals calcify from a semi-isolated calcifying fluid, borate may substitute for the carbonate ion ( $\text{CO}_3^{2-}$ ; Sen et al., 1994). Although there are multiple pathways by which this could occur, recent inorganic precipitation studies (Holcomb et al., 2016) suggest that it likely occurs via de-protonation and co-precipitation with  $\text{CO}_3^{2-}$  (Noireaux et al., 2015), rather than via bicarbonate or some mixture of the two, as previously proposed (Allison et al., 2014).

The initial calcifying fluid  $\delta^{11}\text{B}$  and total boron concentrations are thought to be the same as that of seawater, as seawater serves as the source of boron; further, the boron isotopic composition and concentration remains relatively constant during calcification, due to low partitioning coefficient ( $K_D$ ) of B/Ca between aragonite and seawater (i.e., B is strongly excluded from the skeleton during precipitation, Holcomb et al., 2016). We note that diffusion may violate these assumptions under certain conditions; for example, diffusion of isotopically distinct boric acid may alter the  $\delta^{11}\text{B}$  relative to seawater (Gagnon et al., 2021) or increase boron concentrations relative to seawater when pH is elevated. However, there is no experimental evidence for these confounding factors within tropical, symbiont-bearing coral species; as symbionts provide an additional critical source of DIC to the calcifying fluid, biomineralization processes in symbiont-bearing corals are markedly different from that of the cold-water species for which these limitations have been identified. We therefore follow the approach of other recently published studies in this regard (Chalk et al., 2021; DeCarlo et al., 2018; D’Olivo et al., 2019; Ross et al., 2017, 2019; M. T. McCulloch et al., 2017).

As a result of these processes, the skeletal  $\delta^{11}\text{B}$  reflects the pH of the calcifying fluid ( $\text{pH}_{\text{cf}}$ ), while the [B] reflects both pH and the  $[\text{CO}_3^{2-}]$  (DeCarlo et al., 2018; Holcomb et al., 2016). We calculate  $\text{pH}_{\text{cf}}$  from  $\delta^{11}\text{B}$  of the carbonate skeleton (after Zeebe & Wolf-Gladrow, 2001):

$$\text{pH}_{\text{cf}} = pK_B - \log \left[ \frac{(\delta^{11}\text{B}_{\text{sw}} - \delta^{11}\text{B}_{\text{carb}})}{(\alpha_{(\text{B}3-\text{B}4)} \delta^{11}\text{B}_{\text{carb}} - \delta^{11}\text{B}_{\text{sw}} + 1000(\alpha_{(\text{B}3-\text{B}4)} - 1))} \right], \quad (4)$$

where the  $\delta^{11}\text{B}$  of seawater ( $\delta^{11}\text{B}_{\text{sw}}$ ) was defined as  $39.61\text{\textperthousand}$  (Foster et al., 2010), the boron isotope equilibrium constant ( $\alpha_{(\text{B}3-\text{B}4)}$ ) was set to 1.0272 (Klochko et al., 2006), and the dissociation constant of boric acid ( $pK_B$ ) was calculated from temperature, salinity and pressure (after Dickson, 1990). To standardize methods across cores

(as in situ data is not available for all sites or time periods), we used Li/Mg-derived SSTs and Simple Ocean Data Assimilation (SODA) sea-surface salinity (SSS). We used mean climatological SODA SSS (33.5 PSU) for fossil analyses (prior to the industrial era).

Empirical constraints on the B/Ca partitioning coefficient between aragonite and seawater and its dependency on  $pH_{cf}$  (Holcomb et al., 2016) permit reconstruction of carbonate ion concentration in the calcifying fluid from paired  $\delta^{11}\text{B}$ - $pH_{cf}$  and B/Ca measurements (DeCarlo et al., 2018):

$$K_D \equiv (\text{B/Ca})_{\text{CaCO}_3} \times \frac{[\text{CO}_3^{2-}]_{cf}}{[\text{B}(\text{OH})_4^-]_{cf}}, \quad (5a)$$

$$K_D = 0.002\ 97 \exp(-0.020\ 2[\text{H}^+]_{cf}), \quad (5b)$$

and

$$[\text{CO}_3^{2-}]_{cf} = \frac{K_D \times [\text{B}(\text{OH})_4^-]_{cf}}{(\text{B/Ca})_{\text{CaCO}_3}}, \quad (6)$$

where Equation 5b follows the formulation of M. T. McCulloch et al. (2017). Although there continues to be debate over the best  $K_D$  formulation (DeCarlo et al., 2018), Equation 5b is likely to be most accurate for tropical reef-building corals as it does not include the (Mavromatis et al., 2015) experimental data, which was collected from NaCl solutions (rather than seawater) at very low  $[\text{CO}_3^{2-}]$  relative to that of coral CF.

As reviewed by DeCarlo et al. (2018), uncertainties still remain with regards to the most accurate formulation for  $K_D$  and the degree to which  $\text{Ca}^{2+}$  is upregulated within the cf. We evaluated the sensitivity of our results (see Figures S3 and S4 in Supporting Information S1) to the  $K_D$  formulation, following the equations of Holcomb et al. (2016); M. T. McCulloch et al. (2017); DeCarlo et al. (2018) and the boron systematics package of DeCarlo et al. (2018), as well as using a constant  $K_D$  of 0.002 (after Allison, 2017). Our sensitivity tests show that these uncertainties only marginally impact the absolute magnitude of inferred  $\text{DIC}_{cf}$  and do not influence the relative changes across sites and time periods (the focus of this work). Further, the inferred  $\text{DIC}_{cf}$  upregulation is higher using the  $K_D$  formulation of M. T. McCulloch et al. (2017) (Figure S3 in Supporting Information S1); therefore, our chosen approach produces the most conservative change in  $\text{DIC}_{cf}$  and  $\Omega_{cf}$  under warming and acidification. We similarly test the impact of  $\text{Ca}^{2+}$  upregulation relative to seawater on resulting  $\Omega_{cf}$  calculations. For this, we use the mean and  $\pm 1$  standard deviation from independent micro-sensor measurements (see Sevilgen et al., 2019, Table 1). These sensitivity analyses demonstrate that uncertainties  $\text{Ca}^{2+}$  impact the absolute magnitude of  $\Omega_{cf}$  within colonies (Figure S5 in Supporting Information S1), but not the relative differences among colonies, sites, or time periods (the focus of this study). We therefore utilize the most conservative approach, and report results using a  $\text{Ca}^{2+}$  scaling factor of 1, which is the lower ( $-1\sigma$ ) bound from Sevilgen et al. (2019). Inferred trends in  $\Omega_{cf}$  and calcification would be greater if a constant  $K_D$  or higher  $\text{Ca}^{2+}$  are assumed (Figures S4 and S5 in Supporting Information S1). Therefore, the results reported here are the most conservative estimate of inferred  $\Omega$  and calcification changes from preindustrial to modern conditions.

Dissolved inorganic carbon is calculated from the  $pH_{cf}$  (Equation 4) and  $[\text{CO}_3^{2-}]_{cf}$  (Equation 6) using CO2SYS software (Lewis et al., 1998) and the following constants: carbonate species dissociation (Dickson & Millero, 1987; Mehrbach et al., 1973), borate and sulphate dissociation (Dickson, 1990), and aragonite solubility (Mucci, 1983). Finally, we explore the relationship between pH, DIC and  $\Omega$  of the coral calcifying fluid and Sr/Ca-SST (note: we utilize Sr/Ca-SST as a quasi-independent SST estimate rather than Li/Mg-SST, as the latter was used in Equation 4). Our findings are robust to the paleo-thermometer used to assess the impact of temperature on coral carbonate chemistry (e.g., Figure S8 in Supporting Information S1).

## 2.5. Stable Isotope Geochemistry

Stable oxygen and carbon isotope ratios ( $\delta^{18}\text{O}$  and  $\delta^{13}\text{C}$ ) were analyzed on a Thermo Delta V Plus mass spectrometer, coupled to a Kiel IV carbonate preparation system, in the PACE lab, at the University of Michigan's Earth and Environmental Sciences department. Analyses were performed on splits of the same powders analyzed for trace elemental chemistry and paired  $\delta^{11}\text{B}$ -B/Ca boron systematics. Long-term analytical precision (1  $\sigma$ ) of Luxor

internal carbonate standard was  $0.08\text{\textperthousand}$  for  $\delta^{18}\text{O}$  and  $0.05\text{\textperthousand}$  for  $\delta^{13}\text{C}$ . All new stable isotope data are shown in Figures 4 and S10 in Supporting Information S1.

## 2.6. Statistical Analysis

Ordinary least squares regressions (OLS) were used to assess relationships among geochemical parameters within and among coral colonies, and in upregulation with respect to seawater conditions. First, OLS regressions were performed among reconstructed calcifying fluid and skeletal geochemical parameters (Figures 2, S1, S3–S6, and S8 in Supporting Information S1). ANCOVA and multiple comparisons were then utilized to assess differences in the relationship among groups (i.e., among individual cores, or among fossil Wolf, modern Wolf, and GBR corals). Finally, OLS was utilized to assess the relationship between average upregulation of  $\text{pH}_{\text{cf}}$ ,  $\text{DIC}_{\text{cf}}$ , and  $\Omega_{\text{cf}}$  and seawater chemistry and temperature (Tables S4 and S5 in Supporting Information S1). Confidence intervals (95% CI) were determined from the 5th and 95th percentiles of 1000 random draws of the distribution of upregulation estimates (based on the standard deviation and mean of each record).

## 2.7. Coral Densitometry and Calcification

Skeletal density was measured using a quantitative X-ray scanning method developed at the Australian Institute of Marine Science (Anderson et al., 2017, supplementary methods) alongside six compressed *Porites* sp. powder standards. These standards were used to calibrate X-ray grayscale values to known density, by applying a linear fit between known density (multiplied by thickness) and the natural log of each standard's mean grayscale value. Grayscale values were measured from the background-corrected X-ray positives using Fiji software. Analytical precision of these X-ray density measurements was estimated using an additional standard with a known density ( $2.3977 \text{ g cm}^{-2}$ ) and thickness (6.86 mm) with values within the typical range of massive *Porites* spp. coral slabs. The average density of this quality control standard across all five X-rays used in this study was  $2.3655 \text{ g cm}^{-2}$ ; thus, we report an uncertainty of  $0.043 \text{ g cm}^{-2}$  or 1.8%.

For each core, grayscale values were measured along 4 mm-wide transects on either side of the geochemical transect. We report density values from each transect, as well as the average across both transects (to account for micro-scale variations in density associated with skeletal architecture). For each transect, density was calculated using the standard calibration curve, normalized by slab thickness. Thickness was measured at 0.125 cm increments along two transects, and the average thickness was interpolated to 0.005 cm (the sampling resolution of the X-ray density measurements).

Annual growth metrics (density, extension, and calcification) were calculated from warm season to warm season using annual tie points (Sr/Ca minima, SST maxima). This approach was utilized as the seasonal cycle was more clearly identifiable in the Sr/Ca series (relative to that of the growth series). Extension was calculated as the distance between successive Sr/Ca minima, and calcification as the product of extension and annual average skeletal density.

## 2.8. Seawater Carbonate System

Seawater carbonate chemistry ( $\text{TCO}_2$ , Total Alkalinity [TA],  $\text{pCO}_2$ , pH, and  $\Omega_{\text{arag}}$ ) were obtained from (D. P. Manzello, 2010; Manzello et al., 2014; Humphreys et al., 2018). Briefly, seawater samples were collected during the cool ( $n = 24$ ) and warm ( $n = 21$ ) seasons over multiple years in 500 mL borosilicate glass bottles from 7 study sites throughout the archipelago: (a) Bartolomé, Santiago Island; (b) Santa Fe Island; (c) Punta Bassa, San Cristóbal Island; (d) Punta Pitt, San Cristóbal Island; (e) Devil's Crown, Floreana Island; (f) Gardner Bay, Española Island; and (g) Darwin Island ( $N = 7$ ; summary statistics obtained from Humphreys et al., 2018). Here, we utilize the mean ( $\pm$ standard error of the mean, SEM) values to assess the relationship between  $\text{pH}_{\text{cf}}$  and  $\text{DIC}_{\text{cf}}$  (calculated from paired coral  $\delta^{11}\text{B}$  and B/Ca) and regional changes in the seawater  $\text{CO}_2$  system. However, available measurements are discrete, disjointed snapshots, and therefore lack temporal information with which to identify variability on interannual and longer timescales. Further,  $\Omega_{\text{arag}}$  at Wolf Island is expected to display higher mean values and lower seasonal variability (see Manzello, 2009, Figure 1) than the seawater collection sites of (Manzello, 2010), as upwelling and equatorial undercurrent (EUC) strength and variability are weaker

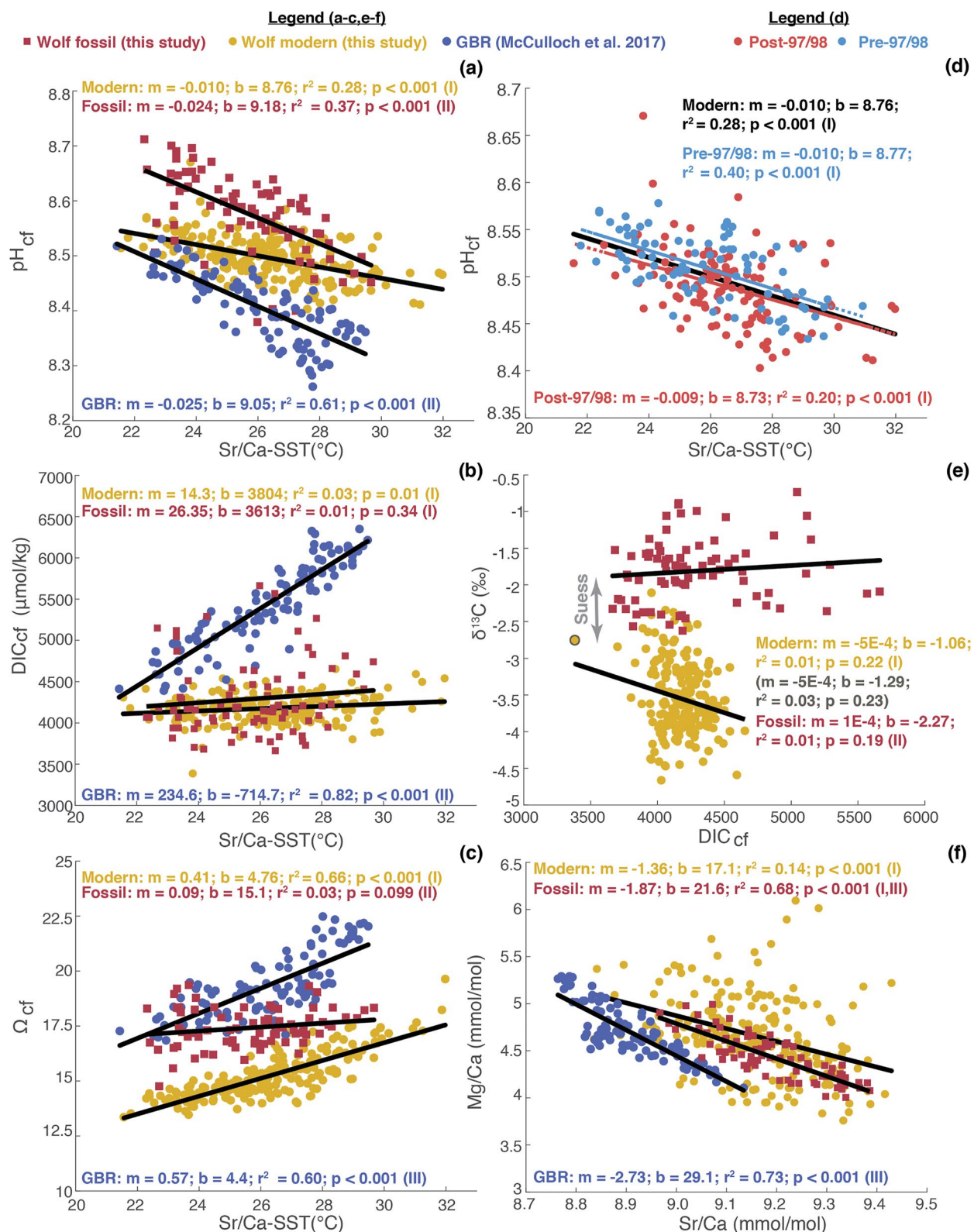


Figure 2.

at Wolf Island. As values from Wolf Island are not publicly available, analyses were performed using both the *in situ* data from Darwin Island (Manzello et al., 2014; Humphreys et al., 2018) and Community Earth System Model version 1 (CESM1).

## 2.9. Community Earth System Model Biogeochemistry

Given the sparse network of seawater inorganic carbon measurements (i.e., DIC, pH, alkalinity) with which to calculate seawater aragonite saturation state, we use the CESM1 Last Millennium Ensemble (LME, Otto-Bliesner et al., 2016) and Large Ensemble (LE, Kay et al., 2015) to compare the chemistry of the coral calcifying fluid to that of local seawater. This approach facilitates comparison across sites, as well as among eighteenth century (LME), twentieth century (LME and LE), and end of 21st century (LE) conditions. The CESM1 marine ecosystem-biogeochemical module (Hurrell et al., 2013) permits analysis of the entire carbonate systems across space and time, permitting the first multi-site, multi-century synthesis of coral calcifying fluid chemistry in response to changing ocean conditions.

The CESM1 LME simulation was validated against OISST SSTs (Reynolds et al., 2007, Figure S2 in Supporting Information S1), SODA SSS (Carton & Giese, 2008, not shown), buoy data (Sutton et al., 2019), seawater samples described above (Table S3 in Supporting Information S1), and the spatially interpolated climatology (1972–2013) from GLODAP version 2 (Lauvset et al., 2016, Table S3 in Supporting Information S1). CESM1 simulated pH and calculated  $\Omega_{sw}$  compare well with the observations across the tropical Pacific, with differences of less than 0.05 and <0.5 (RSDs of <0.6% and 8%), respectively (Table S3 in Supporting Information S1). Further, these discrepancies may be at least partially attributed to the comparison of discrete *in-situ* snapshots of ocean pH with the climatological value over different baseline periods (over which there is a decreasing trend across the tropical Indo-Pacific).

We calculate  $\Omega_{sw}$  from CESM1 LME (full forcing scenario) and LE (Representative Concentration Pathway; RCP8.5) simulated SST, SSS, pH, and DIC using CO2SYS (as described above). Combining the simulated seawater pH, DIC, and  $\Omega$  with boron-derived estimates of coral calcifying fluid pH, DIC, and  $\Omega$ , we estimate the percentage upregulation of calcifying fluid geochemistry. For example, the percent change (henceforth “Pchange”) in aragonite saturation is calculated as:

$$Pchange_{\Omega} = \frac{\Omega_{cf} - \Omega_{sw}}{\Omega_{sw}} \times 100, \quad (7)$$

where  $\Omega_{sw}$  represents the average over the time period overlapping each coral record from CESM1 LME and/or LE.

We perform sensitivity tests at the GBR site, where an *in-situ* seawater timeseries is available, to show that CESM1 LME and LE reproduce the observed Pchange $_{\Omega}$  (i.e., relative to seawater observations) to within  $\pm 26\%$  (LME) and  $\pm 0.5\%$  (LE), respectively (Table S8 in Supporting Information S1). Much of the discrepancy between LME and observed Pchange can be attributed to differences in the time periods of coverage. Therefore, two sensitivity tests were used to assess: (a) the impact of using the annual average, seasonal average (cold vs. warm season), or monthly seawater value, and (b) the impact of using the LME projected values versus using the LE values over the post-2005 interval (i.e., after the final year of the LME). Because the Pchange seasonal variability is dominated by the variability in the coral calcifying fluid (which is  $\gg$  seawater variability), these sensitivity tests demonstrate that there is no difference in the mean Pchange if the average seawater value is used in place of the observed temporal evolution of *in situ*  $\Omega_{sw}$  (M. T. McCulloch et al., 2017). Further, this approach generates the most conservative estimate of the Pchange variability at each site (i.e.,  $1\sigma = 23\& 32\%$ ; Table S8 in Supporting Information S1). The second sensitivity test demonstrated that LE-simulated seawater values displayed the best match with the *in situ* data over the post-2005 period ( $\Delta Pchange_{\Omega} < 0.5\%$ ). Although there are

**Figure 2.** Comparison of the relationships among geochemical proxies, Wolf eighteenth-century fossil (red squares) and modern (twentieth century, orange circles) versus Great Barrier Reef modern (blue circles): (a) Sr/Ca-SST versus  $pH_{cf}$ , (b) Sr/Ca-SST versus DIC $_{cf}$ , (c) Sr/Ca-SST versus  $\Omega_{cf}$ , (e) DIC $_{cf}$  versus  $\delta^{13}\text{C}$  (with and without flier outlined in gray), and (f) Sr/Ca versus Mg/Ca. Comparison of the pre-1997/98 thermal stress (blue), and post-1997/98 thermal stress (red) Sr/Ca-SSTs versus  $pH_{cf}$  for all modern coral data (black) is shown in (d). In all panels, roman numerals (I-III) denote that the slope of the relationship is significantly different from other groups, based on ANCOVA and multiple comparisons (where a significant difference among groups was identified). Groups with the same roman numeral are not significantly different from one another.

no contemporaneous seawater samples collected near Wolf Island,  $\Omega$  Pchange values using seawater data from nearby Darwin (collected in June 2012) are within the  $1\sigma$  range ( $\pm 29\%$ ) of the CESM1-based estimates for WLF10-10a (ending in 2010, Table S9 in Supporting Information S1). We therefore conservatively reported an uncertainty of  $\sim \pm 30\%$  for all  $\text{Pchange}_{\Omega}$  estimates.

We also apply the method of (D’Olivo et al., 2019) to deconvolve the relative contribution of thermodynamics (i.e., SST-driven changes in calcification and/or buffering capacity, Guo, 2019) and  $\text{pH}_{\text{sw}}$  in the observed  $\text{pH}_{\text{cf}}$  trends and seasonal variability. Briefly, we performed a multivariate linear regression between CESM1 simulated temperature and  $\text{pH}_{\text{sw}}$  (independent predictors) and  $\text{pH}_{\text{cf}}$  (dependent predictand). The sensitivity of Wolf coral  $\text{pH}_{\text{cf}}$  to SST and  $\text{pH}_{\text{sw}}$  can be expressed as:

$$\text{pH}_{\text{cf}} = 0.26 \times \text{pH}_{\text{sw}} - 0.0019 \times \text{SST} + 6.34, \quad (8)$$

Similar results were obtained when Sr/Ca-SSTs we used in place of CESM1 simulated SSTs. To quantify the role of SST and  $\text{pH}_{\text{sw}}$  in the observed trends (WLF10-10 and fossil vs. modern) and seasonal variability, we model  $\text{pH}_{\text{cf}}$  from Equation 8 using either (a) the average  $\text{pH}_{\text{sw}}$  and simulated SST, or (b) the average SST and simulated  $\text{pH}_{\text{sw}}$ , respectively.

## 2.10. Predicted Changes in Coral Calcification

Finally, we use the IpHRAC model from (M. McCulloch et al., 2012) to predict the changes in calcification rate ( $G$ ) from  $\Omega_{\text{cf}}$  between time periods (i.e., eighteenth and twentieth):

$$G = k \times (\Omega_{\text{cf}} - 1)^n, \quad (9)$$

where

$$k = -0.0177 \times \text{SST}^2 \quad (10)$$

and

$$n = 0.0628 \times \text{SST} + 0.0985. \quad (11)$$

$\Omega_{\text{cf}}$  is calculated from simulated pH,  $\Omega_{\text{sw}}$ , SST, and SSS and the Pchange (%) upregulation, as described above. Calcification rates are reported as percent changes relative to the baseline period (1970–2005, unless otherwise noted).

## 3. Results and Discussion

### 3.1. Seasonal pH, DIC and $\Omega$ of Coral Calcifying Fluid

Here we compare new reconstructions of SST and calcifying fluid geochemistry (Table S1 in Supporting Information S1) from modern and subfossil Galápagos coral cores with published reconstructions from the GBR (M. T. McCulloch et al., 2017; D’Olivo et al., 2019; Ross et al., 2017). Two eighteenth century coral cores collected at Wolf Island show that as SST increases,  $\text{pH}_{\text{cf}}$  decreases (despite the regional  $\text{pH}_{\text{sw}}$  increase; Figure 2a and Figure S1a in Supporting Information S1). The slope of this relationship (WLF04:  $-0.022$  pH units per  $^{\circ}\text{C}$ ,  $N = 33$ ,  $r^2 = 0.52$ ; WLF05:  $-0.033$  pH units per  $^{\circ}\text{C}$ ,  $N = 45$ ,  $r^2 = 0.43$ ; Figure S1a in Supporting Information S1) is nearly identical to that found among replicate modern corals from the GBR (Davies-02:  $-0.035$  pH units per  $^{\circ}\text{C}$ ,  $N = 50$ ,  $r^2 = 0.82$ ; Davies-03:  $-0.020$  pH units per  $^{\circ}\text{C}$ ,  $N = 54$ ,  $r^2 = 0.80$ ). The seasonal  $\text{pH}_{\text{cf}}$  change is also similar among GBR modern corals and the Wolf fossil coral, with a  $-0.03$  to  $-0.06$  unit change between the average warm and cold seasons (Table S2 in Supporting Information S1) and a range of  $0.2$ – $0.3$  pH units at each site. However, the SST-pH relationship weakens in the two modern (twentieth century) Wolf corals, which display a reduced seasonal pH range ( $\Delta\text{pH} = -0.003$  to  $-0.02$ , Table S2 in Supporting Information S1) and a weaker relationship with temperature (i.e., a shallower slope and lower  $r^2$ ) compared to fossil Wolf cores (Figure S1a in Supporting Information S1).

Comparing the modern and fossil data from Wolf, we demonstrate that the  $\text{pH}_{\text{cf}}$ -SST relationship is significantly weaker in the modern corals than in the fossil corals. In contrast, the Wolf fossil and GBR modern corals are not

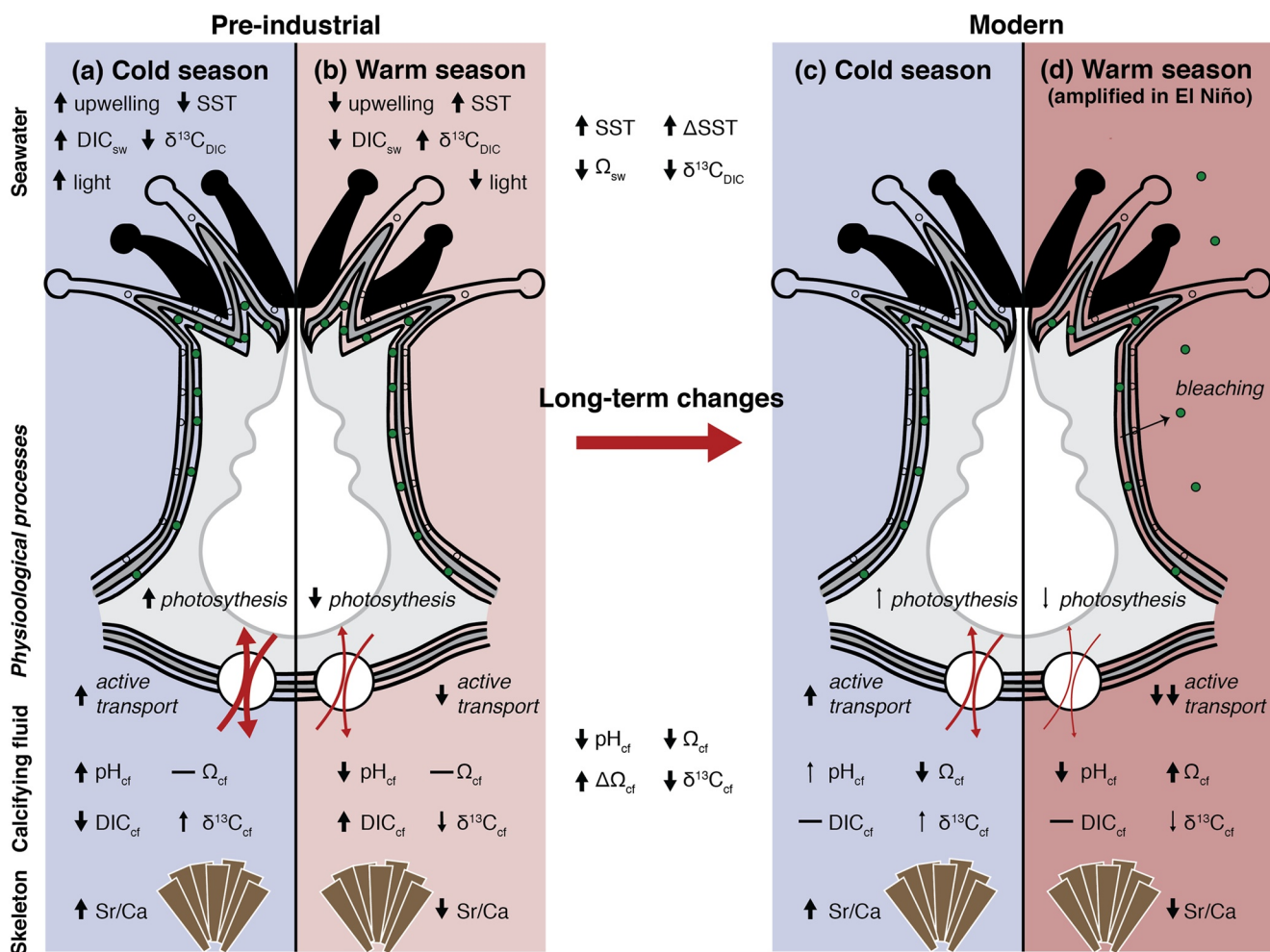


**Figure 3.** Schematic overview of the main seawater and physiological controls (cold season a,c; warm season b,d) on calcifying fluid and skeletal geochemistry in Galapagos eighteenth-century fossil (a-b) and modern (c-d) corals, identified in the current study. Figure 3 modified from (Thompson, 2021), with polyp artwork by E. V. Reed. Arrows indicate the sign of the change, with the thickness indicating the relative magnitude of the change; “—” denote variables with limited to no change.

significantly different from one another (Figure 2a). The greater SST range in modern cores (Figure 2a, *x*-axis) would by itself strengthen this relationship (as in D’Olivo et al., 2019) and therefore cannot explain the observed patterns; we therefore infer that the weakening is likely driven by reduced pH upregulation (Figures 3c and 3d), due to the impacts of OA and/or thermal stress (rather than by temperature-induced changes in calcification or buffering capacity alone Guo, 2019). The difference in slope between the fossil and modern corals equates to 7%–40% difference in H<sup>+</sup> ions in the calcifying fluid (with larger changes at lower temperatures, Figure 2a). As a result, Ω<sub>cf</sub> displays a significant positive relationship with SST in modern Wolf corals (Figures 2c, 3c and 3d), with up to 5% lower saturation during the cold season (September–November; SON) relative to the warm season (Table S2 in Supporting Information S1). In contrast, there is no relationship between Ω<sub>cf</sub> and temperature in the fossil coral (Figures 2c, 3a and 3b) and <1.5% change in Ω<sub>cf</sub> seasonally (Table S2 in Supporting Information S1), though we note that a significant Ω<sub>cf</sub>–temperature relationship is observed in the WLF04 data alone (Figure S1d in Supporting Information S1). These results indicate that the fossil coral maintained a steady aragonite saturation state in its calcifying fluid across seasonally varying environmental conditions, while the modern Wolf corals did not. Put another way, modern Wolf corals appear to have partially lost their ability to buffer calcifying fluid chemistry against changes in seawater pH and Ω. This loss of buffering capacity—shown here for the first time—implies a loss of resilience that is likely to lead to reduced calcification under continued environmental change.

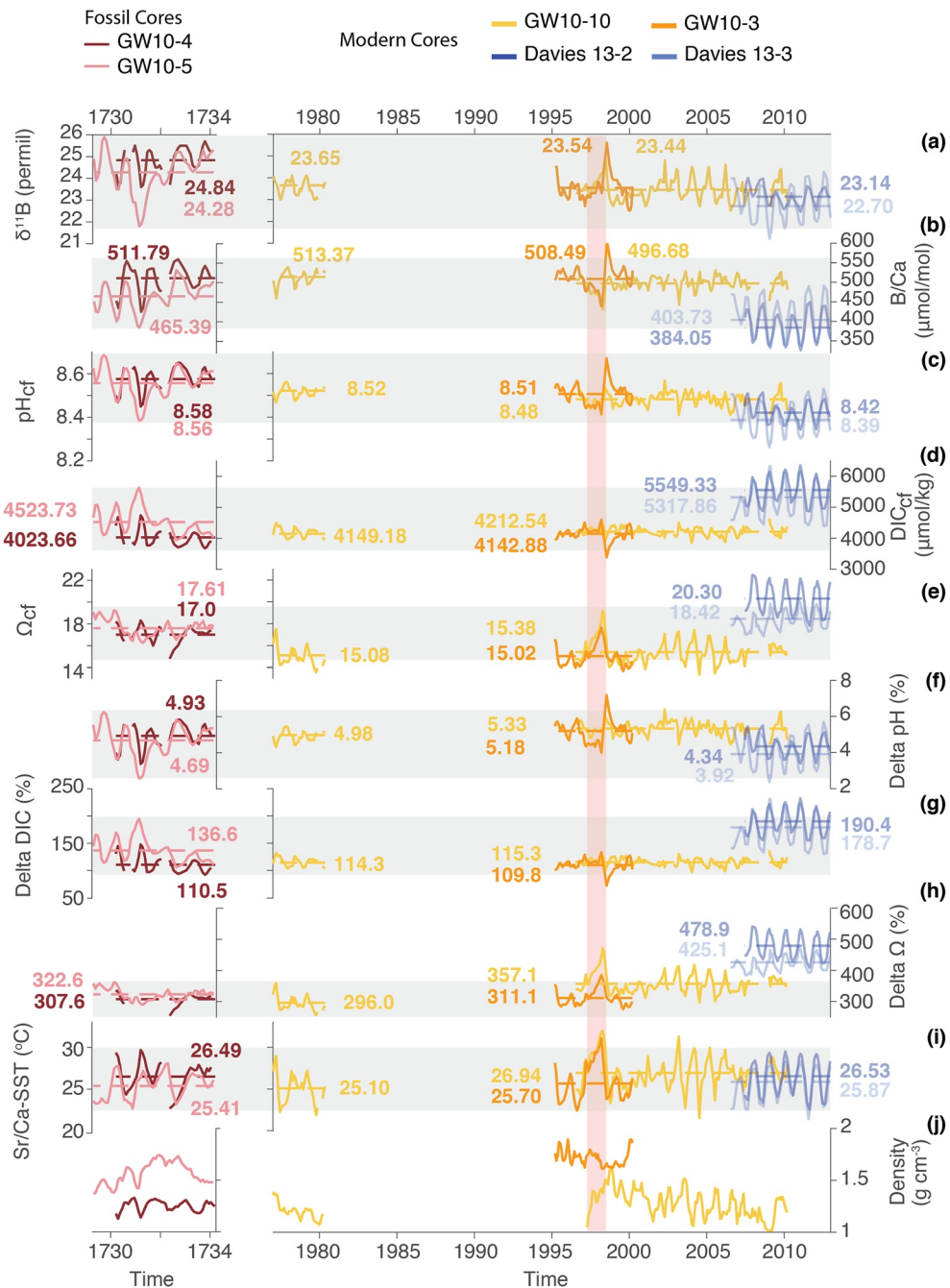


**Figure 4.** Time series of boron-derived calcifying fluid geochemistry, Sr/Ca-SSTs, and skeletal density: Wolf eighteenth-century fossil (red) and modern (twentieth century, orange) versus Great Barrier Reef modern (blue). (a)  $\delta^{11}\text{B}$  (permil), (b) B/Ca ( $\mu\text{mol/mol}$ ), (c)  $\text{pH}_{\text{cf}}$  (total scale), (d)  $\text{DIC}_{\text{cf}}$  ( $\mu\text{mol/kg}$ ), (e)  $\Omega_{\text{cf}}$ , (f) Percent upregulation of  $\text{pH}_{\text{cf}}$  with respect to  $\text{pH}_{\text{sw}}$  (%), (g) Percent upregulation of  $\text{DIC}_{\text{cf}}$  with respect to  $\text{DIC}_{\text{sw}}$  (%), (h) Percent upregulation of  $\Omega_{\text{cf}}$  with respect to  $\Omega_{\text{sw}}$  (%), (i) Sr/Ca-SSTs ( $^{\circ}\text{C}$ ), and (j) skeletal density ( $\text{g cm}^{-3}$ ). See Methods for how these parameters were derived from proxy and model data. Gray shading depicts the range of eighteenth-century fossil geochemical values; red shading depicts warm anomalies associated with the 1997/98 El Niño event; mean geochemical values are denoted by dotted lines on each series.

### 3.2. Reproducibility

The mean and seasonal-interannual variance in calcifying fluid geochemistry were broadly reproducible across cores from both periods (within and among cores at a single site; Table S2 in Supporting Information S1, Figure 4, S1 & S10 in Supporting Information S1). However, an anomalously low  $\delta^{11}\text{B}$  and B/Ca departure in core

WLF05 co-occurring with a low-density and high Sr/Ca-SST anomaly in 1731–1732 emphasizes the need for further work to assess the impact of skeletal density, microstructure (Chalk et al., 2021), and transect quality (Reed et al., 2019, 2021) on skeletal geochemistry within a single colony. Such within colony variations are likely to be more severe at marginal reef sites like the Galápagos Islands, where corals are susceptible to boring bivalves and display lobate growth structure and complex microscale growth features, such as convergent corallite fans, changes in growth direction, and corallites angled relative to the sampling plane (Reed et al., 2021). Nevertheless, outside this short-lived anomaly, the geochemical relationships reported here were reproducible within replicate cores from a single Galápagos fossil coral colony, with no significant differences in slope between the replicate fossil cores (Figure S1 in Supporting Information S1). The only exceptions were the slope of the relationship between  $\delta^{13}\text{C}$  and  $\text{DIC}_{\text{cf}}$  (Figure S1e in Supporting Information S1) and the intercept of the  $\text{DIC}_{\text{cf}}$ -SST relationship (Figure S1b in Supporting Information S1)—suggesting that proxies for metabolic activity may be most susceptible to non-environmental or physiological factors (e.g., skeletal microstructures, overall transect quality, symbiont density and composition, and/or shading within colonies with complex 3D structures), as previously observed for  $\delta^{13}\text{C}$  among transects. Nevertheless, the reproducibility of these relationships suggests that this approach can help expand our knowledge of calcifying fluid geochemistry prior to the industrial era.

Further, sensitivity tests demonstrate that the differences in pH and  $\Omega$  upregulation across sites and time periods are robust regardless of the choice of  $K_D$  and  $[\text{Ca}^{2+}]_{\text{cf}}$  (Figures S3–S5). Further, the values are within the range of those obtained through independent micro-sensor measurements (Sevilgen et al., 2019); recent work comparing  $\delta^{11}\text{B}$ - and microelectrode-based  $\text{pH}_{\text{cf}}$  support the utility of  $\delta^{11}\text{B}$  as a proxy for diurnally averaged  $\text{pH}_{\text{cf}}$  (Guillermic et al., 2020).

### 3.3. Dissolved Inorganic Carbon & $\delta^{13}\text{C}$ Variability

The controls on pH upregulation and  $\text{DIC}_{\text{cf}}$  likely differ across sites. In Australia, seasonal upregulation of  $\text{pH}_{\text{cf}}$  occurs in response to seasonal variations in temperature (Guo, 2019; D’Olivo et al., 2019),  $\text{pH}_{\text{sw}}$  (D’Olivo et al., 2019), and metabolic DIC availability (M. T. McCulloch et al., 2017), with lower DIC during the winter months due to reduced light and cooler temperatures (M. T. McCulloch et al., 2017). This mechanism was proposed in the GBR and Ningaloo Reef, Australia, where both  $\text{DIC}_{\text{cf}}$  (Figures 2b, 3a, 3b, and S1b in Supporting Information S1) and  $\text{DIC}_{\text{cf}}$ /seawater dissolved inorganic carbon ( $\text{DIC}_{\text{sw}}$ ) display a strong positive relationship with temperature (M. T. McCulloch et al., 2017). This pH seasonality is consistent amongst a wide range of reefs, including the GBR, Coral Sea, Western Australia, Caribbean, and Central Pacific (Chalk et al., 2021; D’Olivo & McCulloch, 2017; D’Olivo et al., 2019; Hemming et al., 1998; Knebel et al., 2021; M. T. McCulloch et al., 2017; Pelejero et al., 2005; Ross et al., 2019). However, all of these sites have fundamentally different dynamics than in the Galápagos, where the cool season experiences upwelling of DIC-rich waters (Kessler, 2006, Figures 3a and 3b) that impacts the seasonality of CF chemistry. As a result of these confounding  $\text{DIC}_{\text{sw}}$  and metabolic DIC signals, we find that  $\text{DIC}_{\text{cf}}$  is nearly independent of temperature in modern Wolf corals (Figures 2b, 3c and 3d; though note a very weak positive relationship observed in core WLF03, Figure S1b in Supporting Information S1) and displays a weak positive relationship with temperature in the Wolf fossil coral (Figures 2b, 3a and S1b in Supporting Information S1). Further,  $\text{DIC}_{\text{cf}}$  is upregulated by a near-constant factor of  $\sim 2$  relative to  $\text{DIC}_{\text{sw}}$  in modern Wolf corals, compared with a stronger, seasonally varying  $\text{DIC}_{\text{cf}}$  enrichment in GBR corals ( $\text{DIC}_{\text{cf}}/\text{DIC}_{\text{sw}} = 2.2\text{--}3.2$ , Table S2 in Supporting Information S1) and Galápagos fossil corals.

Comparison of the carbon isotopic ( $\delta^{13}\text{C}$ ) variability among cores may explain why pH regulation is weaker in modern Wolf corals (Figure 2e). First, a relationship between  $\delta^{13}\text{C}$  and the  $\text{DIC}_{\text{cf}}$  in Wolf modern and fossil corals is weak or absent, suggesting that metabolic processes and upwelling contribute approximately equally to the carbon pool at this site. During the cool season, both metabolic processes (which preferentially remove light carbon, enriching the carbon pool and increasing skeletal  $\delta^{13}\text{C}$ ; as reviewed by Swart, 1983) and upwelling (which contributes isotopically light carbon, decreasing skeletal  $\delta^{13}\text{C}$ ) contribute to  $\text{DIC}_{\text{cf}}$ ; therefore the signals compensate, reducing  $\delta^{13}\text{C}$  variance relative to that of  $\text{DIC}_{\text{cf}}$  (e.g., Figure 3a and 3b). Nevertheless, we note a weak negative relationship between  $\delta^{13}\text{C}$  and  $\text{DIC}_{\text{cf}}$  in core WLF03 (Figure S1e in Supporting Information S1), in addition to the consistently more negative  $\delta^{13}\text{C}$  values in the modern samples from the burning of fossil fuels (“Suess effect”; Keeling, 1979). Although additional data are needed to assess the complex interplay of DIC variability at this site, these results suggest that the upwelling of isotopically light carbon is increasingly dominating the  $\text{DIC}_{\text{cf}}$  pool as the seawater DIC pool becomes isotopically lighter and the coral-algae symbiosis becomes increasingly

stressed. Indeed, a significant relationship between  $\delta^{13}\text{C}$  and  $\text{DIC}_{\text{cf}}$  is only present in the post 197/98 data (Figure S6f in Supporting Information S1), driven primarily by large isotopically heavy, low DIC anomalies during and following thermal stress and bleaching.

To assess the strength of DIC upregulation, we use simulated values for seawater carbonate parameters that are unavailable from coral proxies (see Methods), but that compare reasonably well to the limited available direct seawater observations at nearby locations, collected over disparate time periods (Table S3 in Supporting Information S1). We find that Galápagos modern  $\text{DIC}_{\text{cf}}$  never reaches above 2.2 times that of simulated  $\text{DIC}_{\text{sw}}$  ( $\text{DIC}_{\text{cf}}$  max = 4,654  $\mu\text{mol/kg}$  vs.  $\text{DIC}_{\text{sw}}$  max = 2,091  $\mu\text{mol/kg}$ ; Manzello, 2010), whereas the fossil coral  $\text{DIC}_{\text{cf}}$  reaches as much as  $\sim$ 2.8 times that of seawater (5,663  $\mu\text{mol/kg}$ , which is within the range observed at the GBR, Figure 2b). These results are consistent with a larger contribution of metabolic carbon to the DIC pool in the fossil coral (values  $\text{DIC}_{\text{cf}}/\text{DIC}_{\text{sw}} > 1$ ), with large seasonal (Table S2 in Supporting Information S1) and interannual variability (Figure 4d) in  $\text{DIC}_{\text{cf}}$  that reflects the relative strength of upwelling and photosynthetic carbon fixation in response to light and temperature. Further, the weak relationship between  $\text{DIC}_{\text{cf}}$  upregulation and  $\Omega_{\text{sw}}$  across all Wolf corals (Table S4 in Supporting Information S1) suggests that this decrease in  $\text{DIC}_{\text{cf}}$  variability from pre-industrial conditions is likely driven primarily by dysbiosis (i.e., bleaching or loss of healthy coral microbiome and thus a reduction in metabolic carbon) associated with thermal stress, rather than OA. This is consistent with  $\text{DIC}_{\text{cf}}/\text{DIC}_{\text{sw}}$  departures of  $<1$  (i.e., loss of metabolic carbon) during the 1997/98 thermal stress in both modern cores (equating to a 14%–34% reduction in DIC upregulation, Figure 4g). Similar reductions in  $\text{DIC}_{\text{cf}}$  upregulation are observed during other warm extremes in the modern record, whereas DIC upregulation is highest during warm periods in the fossil record. Our results therefore add to the growing body of work identifying adverse effects of thermal stress and bleaching on coral CF chemistry under ocean warming (Cheung et al., 2021; Dishon et al., 2015; D’Olivo & McCulloch, 2017; D’Olivo et al., 2019; Schoepf et al., 2015, 2021). The changes in DIC upregulation identified here imply that extreme thermal stress undermines coral health via photosynthetic reductions that coincide with weak upwelling (and thus feeding capacity); together, these changes deprive the colony of the energy needed to drive the Ca-ATPase pump and/or other active pathways (e.g., other alkalinity pumps or paracellular transport) that upregulate  $\text{pH}_{\text{cf}}$ , leaving them more susceptible to regional changes in  $\text{DIC}_{\text{sw}}$  and  $\text{pH}_{\text{sw}}$ .

Taken together, these results suggest that  $\text{DIC}_{\text{cf}}$  variability in Wolf corals reflects a complex seasonal interplay between upwelling (cold, high  $\text{DIC}_{\text{sw}}$ , low  $\delta^{13}\text{C}_{\text{DIC}}$ ; May–Nov cold season) and photosynthetic/metabolic (warm, high  $\text{DIC}_{\text{cf}}$ , high  $\delta^{13}\text{C}_{\text{cf}}$ ; Dec–April warm season) processes, the latter of which contributes less to the carbon pool in modern Wolf corals. Regional upwelling elevates both concentrations and variability of  $\text{DIC}_{\text{sw}}$ ; these combine with the coral’s metabolic variations to produce fundamentally different  $\text{DIC}_{\text{cf}}$  dynamics at this site relative to the GBR. In other words, in Galápagos corals, pH upregulation is partly driven by variations in the seawater carbon pool, rather than changes in metabolic pathways alone. We thus find that seasonal  $\text{pH}_{\text{cf}}$  variations at Wolf (Table S2 in Supporting Information S1) are driven primarily by seasonal temperature and  $\text{pH}_{\text{sw}}$  variability (e.g., 73% and 33%, respectively, in the longest core WLF10-10; after D’Olivo et al., 2019, see Methods). These results imply that Galápagos corals are more sensitive to environmental drivers, whereas metabolic processes can regulate cf chemistry more strongly in GBR corals.

### 3.4. Temporal Variability in $\text{pH}_{\text{cf}}$ & Impact of Thermal Stress

Comparing the temporal evolution of  $\text{pH}_{\text{cf}}$  among GBR and Wolf corals over the late twentieth century supports our interpretation that corals experience difficulty upregulating  $\text{pH}_{\text{cf}}$  as seawater conditions become less favorable. First, modern Wolf corals display an abrupt drop and subsequent rise in  $\text{pH}_{\text{cf}}$  during and following the 1997/98 El Niño event (Figure 4c), respectively; this event was characterized by extreme temperature anomalies (Cheung et al., 2021; Jimenez et al., 2018; Figure 4i), stress and bleaching (Glynn, 2001). The decrease in  $\text{pH}_{\text{cf}}$  (towards ambient values) likely resulted from a combination of the loss of metabolic DIC from symbiotic photosynthesis (weakening the ability of corals to regulate their internal pH via the Ca-ATPase or other alkalinity pumps), temperature-induced changes in buffering capacity, and the bleaching-related reduction in calcification rate. The latter is supported by the greater change in  $\text{pH}_{\text{cf}}$  in core WLF-3, in which calcification rate declined by 26% in 1998 (Figure S7 in Supporting Information S1). In turn, these changes impact  $\Omega_{\text{cf}}$  regulation (Figures 4e and S6d in Supporting Information S1) and calcification, and thus the imprint of Rayleigh fractionation on the widely utilized Sr/Ca-SST proxy (with less fractionation following bleaching, suggesting a slowdown in calcification, Figure S6h in Supporting Information S1), though Cheung et al. (2021) demonstrate that the Sr/Ca-SST

record at this site is not likely to be influenced by these processes. Therefore, although our results are reproducible among proxy-based and observational SST data (Figures S8 and S9), the breakdown of pH upregulation in modern corals (particularly post-thermal stress and bleaching) may be even greater than indicated by the Sr/Ca-SST proxy records (see Text and Figure S8 in Supporting Information S1).

The full suite of geochemical tracers measured in modern Galápagos corals provides additional support for the thermal sensitivity of active transport pathways (Ca-ATPase pump, other alkalinity pumps, and/or paracellular transport), particularly following the 1997/98 El Niño event (see Text; Figures S6 and S10 in Supporting Information S1). Departures in U/Ca, Mg/Ca, and  $\delta^{13}\text{C}$  suggest changes in  $[\text{CO}_3^{2-}]$ , Rayleigh fractionation, active transport, and photosynthetic activity following acute thermal stress that are consistent with our interpretations from reconstructed Sr/Ca-SST,  $\text{DIC}_{\text{sw}}$  and pH (see Text in Supporting Information S1). For example, the relationship between Sr/Ca and both Mg/Ca and U/Ca weakens significantly after 1997/98, implying weaker Rayleigh fractionation and/or reduced active transport. A weakening of the  $\text{pH}_{\text{cf}}\text{-SST}$  relationship after 1997/98 (Figures 2d and S6a in Supporting Information S1) also supports the hypothesis that corals lose their ability to regulate  $\text{pH}_{\text{cf}}$  via the Ca-ATPase pump or other active pathways post-stress. However, our results are based on relatively few data following this stress event, limiting the significance of these changes (Figure S6a in Supporting Information S1); similar analyses of additional stress events would clarify these patterns and improve interpretations of calcification and skeletal geochemistry following thermal stress and bleaching. Nevertheless, these results are consistent with other recent studies demonstrating acute impacts of thermal stress on  $\text{pH}_{\text{cf}}$  and skeletal geochemistry (Cheung et al., 2021; Clarke et al., 2017, 2019; D'Olivo & McCulloch, 2017; D'Olivo et al., 2019; M. T. McCulloch et al., 2017; Guillermic et al., 2020; Ross et al., 2017; Schoepf et al., 2021).

### 3.5. Limits to Calcifying Fluid Homeostasis

To understand how corals will respond to ongoing and future environmental changes, it is critical to assess the capacity of corals to regulate  $\Omega_{\text{cf}}$  across sites and time periods with different baseline seawater chemistry. Here, we demonstrate that despite large changes in seawater chemistry between the eighteenth century and modern periods inferred from model simulations (Figure 1c), there is no relationship between  $\Omega_{\text{sw}}$  and the upregulation of  $\Omega_{\text{cf}}$  in Galápagos corals (Table S4 in Supporting Information S1). In other words,  $\Omega_{\text{sw}}$  has not had a detectable influence on upregulation capacity, implying that Galápagos corals have not adapted their capacity to regulate  $\Omega_{\text{cf}}$  in response to thermal extremes and OA since the pre-industrial era. Therefore, although they continue to regulate their internal growth environment at maximum capacity, the resulting calcifying fluid saturation levels are significantly lower in modern corals due to OA (Figures 3c and 3d vs. 3a and 3b).

Our results contrast with the apparent pH “homeostasis” observed in extreme environments near submarine seeps in Papua New Guinea (Wall et al., 2016) and Puerto Morelos, Mexico (Wall et al., 2019) and in the Heron Island (GBR) FOCE (Georgiou et al., 2015). At these  $\text{pCO}_2$  extremes, *Porites* spp. corals show a strong relationship between  $\Omega_{\text{cf}}$  upregulation and seawater conditions (e.g.,  $\Delta\Omega_{\text{cf}}$  of 214% and 270% per unit change in  $\Omega_{\text{sw}}$ , respectively, Table S4 in Supporting Information S1). However, in both scenarios,  $\Omega_{\text{sw}}$  was 19%–82% lower than observed on any modern reefs studied here. Further, seep corals have persisted in these conditions for multiple generations and likely have acclimatized and/or adapted to low seawater saturation over long time periods. Therefore, such sites are unlikely to be good analogs for adaptation potential to current rates of OA, which can occur over the lifetime of an individual coral (100+ years). Therefore, despite the potential for acclimation indicated by such studies of extreme conditions, under the real-world environmental change and multivariate stressors, Galápagos *Porites* spp. corals have not demonstrated an ability to adapt to changing pH via  $\text{pH}_{\text{cf}}$  upregulation.

Our synthesis of modern and fossil corals living under contrasting seawater conditions suggests that there may be a physiological limit to the capacity of corals to upregulate  $\text{pH}_{\text{cf}}$  in response to changing ocean conditions and fluctuations in  $\text{DIC}_{\text{cf}}$ . The capacity of corals to upregulate  $\Omega_{\text{cf}}$  is therefore likely to be dictated (to the first order) by their capacity to upregulate  $\text{DIC}_{\text{cf}}$  via metabolic processes (e.g., GBR corals, particularly in the summer months), which we show is reduced both at marginal sites and following bleaching. Galápagos corals, which have low  $\text{DIC}_{\text{cf}}$  *despite* high regional  $\text{DIC}_{\text{sw}}$ , therefore require greater  $\text{pH}_{\text{cf}}$  upregulation than modern GBR *Porites* spp. corals to maintain similar rates of calcification; the limited capacity to upregulate  $\text{pH}_{\text{cf}}$  has therefore reduced  $\Omega_{\text{cf}}$  under modern conditions. Such a physiological limit, if it holds across future acidification (and across additional sites), is likely to leave corals in low-pH, high-DIC environments (i.e., in marginal environments) particularly susceptible to changing ocean saturation.

At both sites, the degree of  $\text{pH}_{\text{cf}}$ ,  $\text{DIC}_{\text{cf}}$ , and  $\Omega_{\text{cf}}$  upregulation relative to seawater varied in concert with SST; warm seasons or years experience greater  $\Omega_{\text{cf}}$  and  $\text{DIC}_{\text{cf}}$  upregulation, and weaker  $\text{pH}_{\text{cf}}$  upregulation (Tables S2 and S5; Figures 4f–4h). These results agree with previous work showing a strong relationship between  $\text{pH}_{\text{cf}}$  upregulation and temperature across a latitudinal gradient (Ross et al., 2019). Physicochemical modeling of coral cf chemistry suggests the temperature dependence of pH upregulation is driven primarily by calcification kinetics, and secondarily by seawater buffering capacity (i.e., the sensitivity of the  $\text{pH}_{\text{cf}}$  to changes in TA; Guo, 2019). This dependence is particularly apparent during the 1997/98 El Niño in Wolf modern corals, with anomalously high  $\text{pH}_{\text{cf}}$  and high  $\Omega_{\text{cf}}$  relative to seawater during and immediately following peak warming (January 1998 to September 1998), potentially due to increased buffering capacity at higher temperatures. However, the increase in  $\text{pH}_{\text{cf}}$  upregulation following peak warming (i.e., during the stress recovery period) implies that other physiological mechanisms must also be at play, such as a change in the refresh rate of the cf or a change in the balance of bicarbonate and carbonate that is transported to the site of calcification (D’Olivo & McCulloch, 2017). Although uncertainties in the fidelity of the Sr/Ca-SST proxy across this thermal stress event may add uncertainty to the SST signal (D’Olivo & McCulloch, 2017), only ~2% of the  $\text{pH}_{\text{cf}}$  anomaly can be explained by SST alone, and the  $\Omega$  upregulation anomaly (i.e., 97/98  $\Delta\Omega$  relative to the colony mean  $\Delta\Omega$ , Figure 4h) is robust between the replicate modern cores (23% and 31%) despite differences in calcification rate between colonies. Nevertheless, similar  $\Omega$  upregulation anomalies does not preclude differences in the relative roles of  $\text{DIC}_{\text{cf}}$  and  $\text{pH}_{\text{cf}}$  in this saturation change (Figure 4). Our results suggest that although the response of metabolic carbon production and/or  $\text{pH}_{\text{cf}}$  to thermal stress varies from colony to colony, the relative change in  $\Omega_{\text{cf}}$  with respect to seawater does not vary significantly among colonies. Again, these results demonstrate strong physiological limits to the corals’ ability to regulate their internal carbonate chemistry, and that this limit is likely an emergent property resulting from the interplay of numerous physiological processes or pathways.

### 3.6. Implications for Calcification Under Warming & Acidification

Our results demonstrate that physiological limitations have already had a pronounced impact on the geochemistry of the calcifying fluid in Galápagos *Porites* sp. corals. The  $\text{pH}_{\text{cf}}$  declined significantly between eighteenth century and modern Wolf corals ( $Z = 24.3$ ,  $N = 108,277$ ,  $p < 0.001$ ), and from 1975 to 2010 in the long modern Wolf (GW10-10) record (with a trend of  $-0.18$  pH units per decade). Over 99.9% of this recent trend (between 1975 and 2010) can be attributed to  $\text{pH}_{\text{sw}}$ , with warming contributing less than 0.3% (after D’Olivo et al., 2019, see methods). The mean  $\text{pH}_{\text{cf}}$  was 8.57 in two eighteenth century fossil cores from one colony ( $N = 78$ ) and 8.50 in the two modern corals ( $N = 203$ , Figure 4, Table S2 in Supporting Information S1). This pre-industrial to modern mean  $\text{pH}_{\text{cf}}$  difference can be attributed some combination of  $\text{pH}_{\text{sw}}$  or SST changes. A large model ensemble of simulated changes between these periods suggests that either  $\text{pH}_{\text{sw}}$  or SST could produce  $\text{pH}_{\text{cf}}$  changes of 0.06–0.07 (see methods). In contrast, the temporal change in  $\text{DIC}_{\text{cf}}$  differs between cores, consistent with a varying role of photosynthesis (and thus metabolic carbon) among (and even within) colonies. The combined impact on cf saturation state was profound, with a significant decline of ~2.3 units between the eighteenth century and late-twentieth century corals ( $Z = 24.2$ ,  $N_{\text{fossil}} = 108$ ,  $N_{\text{modern}} = 277$ ,  $p < 0.001$ ). These results emphasize the importance of extending the existing boron reconstructions across time periods that experienced different seawater chemistry from today. This initial study focused on replicate cores from one colony, and it will be critical to further replicate and extend these analyses to other fossil colonies to confirm these findings (given the potential for within and among colony differences in boron geochemistry, e.g., Chalk et al., 2021). Nevertheless, the first such application of boron systematics to pre-industrial fossil coral samples, presented here, paints a potentially stark future under projected acidification, with limited adaptive capacity in the upregulation of the coral calcifying fluid.

Despite this reduction in  $\text{pH}_{\text{cf}}$  between the eighteenth and twentieth century Galápagos corals, there was no significant change in calcification or skeletal density among cores (or between modern and fossil colonies; see section “Coral densitometry and calcification” for description of methods). This is in contrast to previous work that demonstrates a strong relationship between calcification and  $\text{pH}_{\text{cf}}$  (Guillermic et al., 2020; Ross et al., 2019). Rather, we find large interannual changes in calcification rate within (15%–27%) and among (24%–27%) cores (Table S6 and Figure S7 in Supporting Information S1). The predicted change in calcification between the eighteenth and twentieth centuries (of  $-10\%$ ), using simulated  $\Omega_{\text{sw}}$  from Figure 1c, the  $\Omega_{\text{cf}}$  Pchange from Table S4 in Supporting Information S1 and the model of M. McCulloch et al. (2012), therefore falls within the range of interannual calcification variability at this site. Thus, despite large declines in  $\Omega_{\text{cf}}$ , the impact on coral calcification is not yet detectable at Wolf Island, Galápagos given the high interannual calcification variability.

However, these results should not be interpreted as evidence that Galápagos corals are robust to changing ocean chemistry, for five reasons. First, monthly skeletal density data is strongly related to both CF saturation state and temperature in both fossil and modern Galápagos corals (Figure 4). Although the nature of these relationships vary across cores (see Table S7 in Supporting Information S1; e.g., as a function of colony-to-colony variations in bleaching susceptibility), the relationships indicate declining density with warming and lower cf saturation (except in core WLF-3) and an increasing importance of warming in recent decades (becoming the dominant predictor in core WLF-10a, ending in 2010). Second, the corals studied here are likely to represent the “best-case-scenario,” as these long-lived corals targeted for paleoclimate reconstructions are the “winners” that were able to maintain rapid upward extension and calcification despite thermal stress (1997/98) and acidification (Figure S7 in Supporting Information S1). In smaller *P. lobata* colonies at nearby Darwin Island (Manzello et al., 2014), calcification rates were less than half those measured in our longer Wolf cores, despite similar density values among colonies from both sites (Table S6 in Supporting Information S1). Further, the modern Wolf colonies regrew in 3.4 (WLF10-10) and 5 (WLF10-03) years following the very strong 1982/83 El Niño event that devastated reefs across the Galápagos (Glynn et al., 1988), suggesting they experienced only partial mortality during this extreme event. Both colonies also displayed only modest reductions in extension and calcification during or following the 1997/98 event (Figure S7 in Supporting Information S1). Because paleoclimate records are biased towards corals that survive, they likely yield a conservative (i.e., too-stable) estimates of past calcification changes. Third, observed and simulated ocean pH at Galápagos remained above 8.0 over this period (mean CESM1 = 8.08–8.11 over intervals of coral coverage; Darwin = 8.07, Humphreys et al., 2018), a critical tipping point below which corals across the archipelago suffer reduced calcification and structural persistence (Manzello et al., 2014). High nutrients (Manzello et al., 2014) and variable seawater conditions exacerbate the stressful impacts of acidification in upwelling regions, resulting in tipping points at higher pH values (Manzello et al., 2014). Fourth, the temperature dependence of calcification kinetics does not appear to compensate for the impacts of saturation-state changes at Wolf (unlike in more optimal environments; Burton & Walter, 1987; Lough & Barnes, 2000). Lastly, and critically, we demonstrate that as oceans acidify, Wolf corals have not intensified their upregulation of pH or  $\Omega$ , suggesting that continued OA is likely to have significant impacts on calcification at this site.

Finally, our results support the potential to reconstruct changes in paleo-pH from the geochemistry of coral calcifying fluid. Consistent with recent studies (Guo, 2019; D’Olivo et al., 2019), the narrow range in  $\text{pH}_{\text{cf}}$  upregulation of *Porites* spp. across sites and time periods (Table S4 in Supporting Information S1) suggests that within this paleo-relevant genus, long-term  $\text{pH}_{\text{cf}}$  trends are primarily driven by  $\text{pH}_{\text{sw}}$  and not physiological controls (which regulate calcifying fluid chemistry on seasonal timescales, in response to temperature-related changes in DIC, calcification, and buffering capacity). Physiological limits in this capacity to regulate  $\text{pH}_{\text{cf}}$ —identified here for the first time—suggest that as seawater saturation shifts to lower values (as observed with OA, or across spatial gradients, Manzello et al., 2014), so will the distribution of carbonate saturation in the calcifying fluid (as observed between eighteenth and twentieth corals). Corals’ capacity to buffer against OA may therefore be more limited than predicted from experimental manipulations and extreme environments (CO<sub>2</sub> seeps), with particularly severe consequences for corals at marginal sites characterized by reduced metabolic carbon production, low seawater pH, and frequent or severe thermal stress.

#### 4. Summary

In presenting the first analysis of calcifying fluid geochemistry in pre-industrial and modern corals from a marginal environment, we are able to reconcile two seemingly competing truths about the capacity for corals to buffer against changing environmental conditions. On the one hand, we provide further evidence that corals are able to strongly upregulate the pH of their internal growth medium to maintain supersaturation in response to seasonal changes in DIC and temperature. This physiologically driven seasonal upregulation of  $\text{pH}_{\text{cf}}$  precludes the use of boron isotope geochemistry for reconstructing short-term variations in paleo-pH<sub>sw</sub>, but suggests that corals may be able to buffer against changing ocean conditions and maintain calcification under future warming and OA. On the other hand, recent work suggests that long-term trends in  $\text{pH}_{\text{cf}}$  inferred from boron isotope geochemistry are driven primarily by  $\text{pH}_{\text{sw}}$  (D’Olivo et al., 2019), suggesting at least some sensitivity to environmental conditions. However, the resource-intensive nature of boron isotope geochemistry has limited the production of long reconstructions with which to assess corals’ buffering capacity under changing ocean conditions and therefore corals’ resilience to future warming and acidification.

Using cores from a pre-industrial fossil and two modern coral colonies from the Galápagos Islands—a marginal environment characterized by high environmental variability, low seawater pH, and frequent thermal stress—we identify significant declines in  $\text{pH}_{\text{cf}}$  and  $\Omega_{\text{cf}}$  with warming and OA since the pre-industrial period. These trends are exacerbated during and after thermal stress events observed in the modern corals, likely due to the impact of bleaching on metabolic DIC production and the energy-intensive active transport that concentrates alkalinity against the electrochemical gradients. Critically, we demonstrate that these changes may be attributed to a remarkably narrow range of  $\text{pH}_{\text{cf}}$  upregulation across sites and time periods, suggesting a strict physiological limit in corals' ability to regulate their internal carbonate chemistry. We therefore find that the capacity of corals to maintain stable  $\Omega_{\text{cf}}$  supersaturation is dictated (to the first order) by their capacity to upregulate  $\text{DIC}_{\text{cf}}$  via metabolic processes, which is reduced both at marginal sites and following bleaching. Such physiological limits in this capacity to regulate  $\text{pH}_{\text{cf}}$ —identified here for the first time—suggest that corals' capacity to buffer against OA may be more limited than predicted from experimental manipulations and extreme environments (e.g.,  $\text{CO}_2$  seeps). These findings have particularly severe consequences for coral calcification and thus reef structure and function at marginal sites.

## Conflict of Interest

The authors declare no conflicts of interest relevant to this study.

## Data Availability Statement

All geochemical data is publicly available on the National Center for Environmental Information (formerly the National Climatic Data Center) paleoclimatology database: <https://www.nci.noaa.gov/access/paleo-search/study/35193>.

## Acknowledgments

We thank the Charles Darwin Station and the Parque Nacional Galápagos, particularly Galo Quezada, for field work support and permitting for coral collection. We also thank Colin Chilcott, Meriwether Wilson, Roberto Pepolás, Diego Ruiz, Jenifer Suarez, and the captain and crew of the Queen Mabel for their assistance in the field. This work is supported by National Science Foundation grants 1401326/1829613 and 0957881 to Julia E. Cole; UK Natural Environment Research Council grant NE/H009957/1 to A. W. Tudhope; University of Arizona Honors College Alumni Legacy Grant to A. H. Cheung; ARC Centre of Excellence grant CE140100020 to MM and J. P. D'Olivo; and startup funds awarded to D. Thompson from Boston University. AIMS is a federally funded government research agency. This publication is contribution number 2434 of the Charles Darwin Foundation for the Galapagos Islands.

## References

- Allison, N. (2017). Reconstructing coral calcification fluid dissolved inorganic carbon chemistry from skeletal boron: An exploration of potential controls on coral aragonite B/Ca. *Heliyon*, 3(8), e00387. <https://doi.org/10.1016/j.heliyon.2017.e00387>
- Allison, N., Cohen, I., Finch, A. A., Erez, J., & Tudhope, A. W. (2014). Corals concentrate dissolved inorganic carbon to facilitate calcification. *Nature Communications*, 5(1), 1–6. <https://doi.org/10.1038/ncomms6741>
- Anderson, K. D., Cantin, N. E., Heron, S. F., Pisapia, C., & Pratchett, M. S. (2017). Variation in growth rates of branching corals along Australia's Great Barrier Reef. *Scientific Reports*, 7(1), 1–13. <https://doi.org/10.1038/s41598-017-03085-1>
- Beck, J. W., Edwards, R. L., Ito, E., Taylor, F. W., Recy, J., Rougerie, F., et al. (1992). Sea-surface temperature from coral skeletal strontium/calcium ratios. *Science*, 257(5070), 644–647. <https://doi.org/10.1126/science.257.5070.644>
- Burton, E. A., & Walter, L. M. (1987). Relative precipitation rates of aragonite and Mg calcite from seawater: Temperature or carbonate ion control? *Geology*, 15(2), 111–114. [https://doi.org/10.1130/0091-7613\(1987\)15<111:rpaao>2.0.co;2](https://doi.org/10.1130/0091-7613(1987)15<111:rpaao>2.0.co;2)
- Carton, J. A., & Giese, B. S. (2008). A reanalysis of ocean climate using Simple Ocean Data Assimilation (SODA). *Monthly Weather Review*, 136(8), 2999–3017. <https://doi.org/10.1175/2007mwr1978.1>
- Chalk, T., Standish, C., D'Angelo, C., Castillo, K., Milton, J., & Foster, G. (2021). Mapping coral calcification strategies from in situ boron isotope and trace element measurements of the tropical coral *Siderastrea siderea*. *Scientific Reports*, 11. <https://doi.org/10.1038/s41598-020-78778-1>
- Cheng, H., Edwards, R. L., Shen, C.-C., Polyak, V. J., Asmerom, Y., Woodhead, J., et al. (2013). Improvements in  $^{230}\text{Th}$  dating,  $^{230}\text{Th}$  and  $^{234}\text{U}$  half-life values, and U-Th isotopic measurements by multi-collector inductively coupled plasma mass spectrometry. *Earth and Planetary Science Letters*, 371, 82–91. <https://doi.org/10.1016/j.epsl.2013.04.006>
- Cheung, A. H., Cole, J. E., Thompson, D. M., Vetter, L., Jimenez, G., & Tudhope, A. W. (2021). Fidelity of the coral Sr/Ca paleothermometer following heat stress in the northern Galápagos. *Paleoceanography and Paleoclimatology*, 36, e2021PA004323. <https://doi.org/10.1029/2021PA004323>
- Clarke, H., D'Olivo, J., Conde, M., Evans, R., & McCulloch, M. (2019). Coral records of variable stress impacts and possible acclimatization to recent marine heat wave events on the Northwest shelf of Australia. *Paleoceanography and Paleoclimatology*, 34(11), 1672–1688. <https://doi.org/10.1029/2018pa003509>
- Clarke, H., D'Olivo, J. P., Falter, J., Zinke, J., Lowe, R., & McCulloch, M. (2017). Differential response of corals to regional mass-warming events as evident from skeletal Sr/Ca and Mg/Ca ratios. *Geochemistry, Geophysics, Geosystems*, 18(5), 1794–1809. <https://doi.org/10.1002/2016gc006788>
- Corrège, T., Delcroix, T., Récy, J., Beck, W., Cabioch, G., & Le Corne, F. (2000). Evidence for stronger El Niño-Southern Oscillation (ENSO) events in a mid-Holocene massive coral. *Paleoceanography*, 15(4), 465–470. <https://doi.org/10.1029/1999pa000409>
- Cortés, J. (1997). Biology and geology of eastern pacific coral reefs. *Coral Reefs*, 16(1), S39–S46. <https://doi.org/10.1007/s003380050240>
- Cuny-Guirriec, K., Douville, E., Reynaud, S., Allemand, D., Bordier, L., Canesi, M., et al. (2019). Coral Li/Mg thermometry: Caveats and constraints. *Chemical Geology*, 523, 162–178. <https://doi.org/10.1016/j.chemgeo.2019.03.038>
- Darwin, C., & Bonney, T. G. (1889). *The structure and distribution of coral reefs*. Smith.
- DeCarlo, T. M., Gaetani, G. A., Holcomb, M., & Cohen, A. L. (2015). Experimental determination of factors controlling U/Ca of aragonite precipitated from seawater: Implications for interpreting coral skeleton. *Geochimica et Cosmochimica Acta*, 162, 151–165. <https://doi.org/10.1016/j.gca.2015.04.016>

- DeCarlo, T. M., Holcomb, M., & McCulloch, M. T. (2018). Reviews and syntheses: Revisiting the boron systematics of aragonite and their application to coral calcification. *Biogeosciences*, 15(9), 2819–2834. <https://doi.org/10.5194/bg-15-2819-2018>
- Dickson, A. G. (1990). Thermodynamics of the dissociation of boric acid in synthetic seawater from 273.15 to 318.15 K. Deep Sea Research Part A. *Oceanographic Research Papers*, 37(5), 755–766. [https://doi.org/10.1016/0198-0149\(90\)90004-f](https://doi.org/10.1016/0198-0149(90)90004-f)
- Dickson, A. G., & Millero, F. J. (1987). A comparison of the equilibrium constants for the dissociation of carbonic acid in seawater media. *Deep Sea Research Part A. Oceanographic Research Papers*, 34(10), 1733–1743. [https://doi.org/10.1016/0198-0149\(87\)90021-5](https://doi.org/10.1016/0198-0149(87)90021-5)
- Dishon, G., Fisch, J., Horn, I., Kaczmarek, K., Bijma, J., Gruber, D. F., et al. (2015). A novel paleo-bleaching proxy using boron isotopes and high-resolution laser ablation to reconstruct coral bleaching events. *Biogeosciences*, 12(19), 5677–5687. <https://doi.org/10.5194/bg-12-5677-2015>
- D'Olivo, J. P., Ellwood, G., DeCarlo, T. M., & McCulloch, M. T. (2019). Deconvolving the long-term impacts of ocean acidification and warming on coral biomineralisation. *Earth and Planetary Science Letters*, 526, 115785. <https://doi.org/10.1016/j.epsl.2019.115785>
- D'Olivo, J. P., & McCulloch, M. (2017). Response of coral calcification and calcifying fluid composition to thermally induced bleaching stress. *Scientific Reports*, 7(1), 1–15.
- D'Olivo, J. P., Sinclair, D. J., Rankenburg, K., & McCulloch, M. T. (2018). A universal multi-trace element calibration for reconstructing sea surface temperatures from long-lived *Porites* corals: Removing 'vital-effects'. *Geochimica et Cosmochimica Acta*, 239, 109–135. <https://doi.org/10.1016/j.gca.2018.07.035>
- Edwards, R. L., Chen, J., & Wasserburg, G. (1987).  $^{238}\text{U}$ - $^{234}\text{U}$ - $^{230}\text{Th}$ - $^{226}\text{Ra}$  systematics and the precise measurement of time over the past 500,000 years. *Earth and Planetary Science Letters*, 81(2–3), 175–192. [https://doi.org/10.1016/0012-821x\(87\)90154-3](https://doi.org/10.1016/0012-821x(87)90154-3)
- Foster, G., Pogge von Strandmann, P. A., & Rae, J. (2010). Boron and magnesium isotopic composition of seawater. *Geochemistry, Geophysics, Geosystems*, 11(8), Q08015. <https://doi.org/10.1029/2010gc003201>
- Gagnon, A. C., Gothmann, A. M., Branson, O., Rae, J. W., & Stewart, J. A. (2021). Controls on boron isotopes in a cold-water coral and the cost of resilience to ocean acidification. *Earth and Planetary Science Letters*, 554, 116662. <https://doi.org/10.1016/j.epsl.2020.116662>
- Gattuso, J.-P., Kirkwood, W., Barry, J., Cox, E., Gazeau, F., Hansson, L., et al. (2014). Free-ocean  $\text{CO}_2$  enrichment (FOCE) systems: Present status and future developments. *Biogeosciences*, 11(15), 4057–4075. <https://doi.org/10.5194/bg-11-4057-2014>
- Georgiou, L., Falter, J., Trotter, J., Kline, D. I., Holcomb, M., Dove, S. G., et al. (2015). pH homeostasis during coral calcification in a free ocean  $\text{CO}_2$  enrichment (FOCE) experiment, Heron Island reef flat, Great Barrier Reef. *Proceedings of the National Academy of Sciences*, 112(43), 13219–13224. <https://doi.org/10.1073/pnas.1505586112>
- Glynn, P. W. (2001). Eastern Pacific coral reef ecosystems. In *Coastal marine ecosystems of Latin America* (pp. 281–305). Springer. [https://doi.org/10.1007/978-3-662-04482-7\\_20](https://doi.org/10.1007/978-3-662-04482-7_20)
- Glynn, P. W., Alvarado, J. J., Banks, S., Cortés, J., Feingold, J. S., Jiménez, C., et al. (2017). Eastern Pacific coral reef provinces, coral community structure and composition: An overview. In *Coral reefs of the eastern tropical Pacific* (pp. 107–176). Springer. [https://doi.org/10.1007/978-94-017-7499-4\\_5](https://doi.org/10.1007/978-94-017-7499-4_5)
- Glynn, P. W., Cortés-Núñez, J., Guzmán-Espinal, H. M., & Richmond, R. H. (1988). El Niño (1982–83) associated coral mortality and relationship to sea surface temperature deviations in the tropical eastern Pacific. Mortalidad de corales asociada con El Niño (1982–83) y relación con las desviaciones de la temperatura superficial del mar en el Pacífico oriental tropical. In *Proceedings of the 6th International Coral Reef Symposium, Australia* (Vol. 3, pp. 237–243).
- Glynn, P. W., Feingold, J. S., Baker, A., Banks, S., Baums, I. B., et al. (2018). State of corals and coral reefs of the Galápagos Islands (Ecuador): Past, present and future. *Marine Pollution Bulletin*, 133, 717–733. <https://doi.org/10.1016/j.marpolbul.2018.06.002>
- Guillermic, M., Cameron, L. P., De Corte, I., Misra, S., Bijma, J., de Beer, D., & Eagle, R. A. (2020). Thermal stress reduces pocilloporid coral resilience to ocean acidification by impairing control over calcifying fluid chemistry. *Science Advances*, 7(2), eaba9958. <https://www.science.org/doi/10.1126/sciadv.aba9958>
- Guo, W. (2019). Seawater temperature and buffering capacity modulate coral calcifying pH. *Scientific Reports*, 9(1), 1–13. <https://doi.org/10.1038/s41598-018-36817-y>
- Gutjahr, M., Bordier, L., Douville, E., Farmer, J., Foster, G. L., Hathorne, E. C., et al. (2021). Sub-per mil interlaboratory consistency for solution-based boron isotope analyses on marine carbonates. *Geostandards and Geoanalytical Research*, 45(1), 59–75. <https://doi.org/10.1111/gr.12364>
- Hathorne, E. C., Felis, T., Suzuki, A., Kawahata, H., & Cabioch, G. (2013). Lithium in the aragonite skeletons of massive *Porites* corals: A new tool to reconstruct tropical sea surface temperatures. *Paleoceanography*, 28(1), 143–152. <https://doi.org/10.1029/2012pa002311>
- Hathorne, E. C., Gagnon, A., Felis, T., Adkins, J., Asami, R., Boer, W., et al. (2013). Interlaboratory study for coral Sr/Ca and other element/Ca ratio measurements. *Geochemistry, Geophysics, Geosystems*, 14(9), 3730–3750. <https://doi.org/10.1029/ggpe.20230>
- Hemming, N., Guilderson, T., & Fairbanks, R. (1998). Seasonal variations in the boron isotopic composition of coral: A productivity signal? *Global Biogeochemical Cycles*, 12(4), 581–586. <https://doi.org/10.1029/98gb02337>
- Holcomb, M., DeCarlo, T., Gaetani, G., & McCulloch, M. (2016). Factors affecting B/Ca ratios in synthetic aragonite. *Chemical Geology*, 437, 67–76. <https://doi.org/10.1016/j.chemgeo.2016.05.007>
- Holcomb, M., DeCarlo, T., Schoepf, V., Dissard, D., Tanaka, K., & McCulloch, M. (2015). Cleaning and pre-treatment procedures for biogenic and synthetic calcium carbonate powders for determination of elemental and boron isotopic compositions. *Chemical Geology*, 398, 11–21. <https://doi.org/10.1016/j.chemgeo.2015.01.019>
- Humphreys, A. F., Halfar, J., Ingle, J. C., Manzello, D., Reymond, C. E., Westphal, H., & Riegl, B. (2018). Effect of seawater temperature, pH, and nutrients on the distribution and character of low abundance shallow water benthic foraminifera in the Galápagos. *PLoS One*, 13(9). <https://doi.org/10.1371/journal.pone.0202746>
- Hurrell, J. W., Holland, M. M., Gent, P. R., Ghan, S., Kay, J. E., Kushner, P., et al. (2013). The community earth system model: A framework for collaborative research. *Bulletin of the American Meteorological Society*, 94(9), 1339–1360. <https://doi.org/10.1175/bams-d-12-00121.1>
- Jimenez, G., Cole, J. E., Thompson, D. M., & Tudhope, A. W. (2018). Northern Galápagos corals reveal twentieth century warming in the eastern tropical Pacific. *Geophysical Research Letters*, 45(4), 1981–1988. <https://doi.org/10.1002/2017gl075323>
- Kay, J. E., Deser, C., Phillips, A., Mai, A., Hannay, C., Strand, G., et al. (2015). The Community Earth System Model (CESM) large ensemble project: A community resource for studying climate change in the presence of internal climate variability. *Bulletin of the American Meteorological Society*, 96(8), 1333–1349. <https://doi.org/10.1175/bams-d-13-00255.1>
- Keeling, C. D. (1979). The Suess effect:  $^{13}\text{C}$ - $^{14}\text{C}$  interrelations. *Environment International*, 2(4–6), 229–300. [https://doi.org/10.1016/0160-4120\(79\)90005-9](https://doi.org/10.1016/0160-4120(79)90005-9)
- Kessler, W. S. (2006). The circulation of the eastern tropical Pacific: A review. *Progress in Oceanography*, 69(2–4), 181–217. <https://doi.org/10.1016/j.pocean.2006.03.009>

- Klochko, K., Kaufman, A. J., Yao, W., Byrne, R. H., & Tossell, J. A. (2006). Experimental measurement of boron isotope fractionation in seawater. *Earth and Planetary Science Letters*, 248(1–2), 276–285. <https://doi.org/10.1016/j.epsl.2006.05.034>
- Knebel, O., Carvajal, C., Standish, C. D., Vega, E. d. l., Chalk, T. B., Ryan, E. J., & Kench, P. (2021). *Porites* calcifying fluid pH on seasonal to diurnal scales. *Journal of Geophysical Research: Oceans*, 126(3), e2020JC016889. <https://doi.org/10.1029/2020JC016889>
- Lauvset, S. K., Key, R. M., Olsen, A., van Heuven, S., Velo, A., Lin, X., et al. (2016). A new global interior ocean mapped climatology: The 1° × 1° GLODAP version 2. *Earth System Science Data*, 8, 325–340. <https://doi.org/10.5194/essd-8-325-2016>
- Lea, D. W., Shen, G. T., & Boyle, E. A. (1989). Coralline barium records temporal variability in equatorial Pacific upwelling. *Nature*, 340(6232), 373–376. <https://doi.org/10.1038/340373a0>
- Lewis, E., Wallace, D., & Allison, L. J. (1998). Program developed for CO<sub>2</sub> system calculations (Technical Report). Brookhaven National laboratory. Department of Applied Science. <https://doi.org/10.2172/639712>
- Lough, J. M., & Barnes, D. (2000). Environmental controls on growth of the massive coral *Porites*. *Journal of Experimental Marine Biology and Ecology*, 245(2), 225–243. [https://doi.org/10.1016/s0022-0981\(99\)00168-9](https://doi.org/10.1016/s0022-0981(99)00168-9)
- Lough, J. M. (2010). Climate records from corals. *Wiley Interdisciplinary Reviews: Climate Change*, 1(3), 318–331. <https://doi.org/10.1002/wcc.39>
- Manzello, D. P. (2009). Reef development and resilience to acute (El Niño warming) and chronic (high-CO<sub>2</sub>) disturbances in the eastern tropical Pacific: A real-world climate change model. *Proceedings of the 11th International Coral Reef Symposium*, 1, 1299–1304.
- Manzello, D. P. (2010). Ocean acidification hotspots: Spatiotemporal dynamics of the seawater CO<sub>2</sub> system of eastern Pacific coral reefs. *Limnology & Oceanography*, 55(1), 239–248. <https://doi.org/10.4319/lo.2010.55.1.0239>
- Manzello, D. P., Enochs, I. C., Bruckner, A., Renaud, P. G., Kolodziej, G., Budd, D. A., et al. (2014). Galápagos coral reef persistence after ENSO warming across an acidification gradient. *Geophysical Research Letters*, 41(24), 9001–9008. <https://doi.org/10.1002/2014gl062501>
- Manzello, D. P., Kleypas, J. A., Budd, D. A., Eakin, C. M., Glynn, P. W., & Langdon, C. (2008). Poorly cemented coral reefs of the eastern tropical Pacific: Possible insights into reef development in a high-CO<sub>2</sub> world. *Proceedings of the National Academy of Sciences*, 105(30), 10450–10455. <https://doi.org/10.1073/pnas.0712167105>
- Mavromatis, V., Montouillout, V., Noireaux, J., Gaillardet, J., & Schott, J. (2015). Characterization of boron incorporation and speciation in calcite and aragonite from co-precipitation experiments under controlled pH, temperature and precipitation rate. *Geochimica et Cosmochimica Acta*, 150, 299–313. <https://doi.org/10.1016/j.gca.2014.10.024>
- McConaughay, T. (1989). <sup>13</sup>C and <sup>18</sup>O isotopic disequilibrium in biological carbonates: II. In vitro simulation of kinetic isotope effects. *Geochimica et Cosmochimica Acta*, 53(1), 163–171. [https://doi.org/10.1016/0016-7037\(89\)90283-4](https://doi.org/10.1016/0016-7037(89)90283-4)
- McCulloch, M., Falter, J., Trotter, J., & Montagna, P. (2012). Coral resilience to ocean acidification and global warming through pH up-regulation. *Nature Climate Change*, 2(8), 623–627. <https://doi.org/10.1038/nclimate1473>
- McCulloch, M. T., D'Olivo, J. P., Falter, J., Holcomb, M., & Trotter, J. A. (2017). Coral calcification in a changing world and the interactive dynamics of pH and DIC upregulation. *Nature Communications*, 8(1), 1–8. <https://doi.org/10.1038/ncomms15686>
- McCulloch, M. T., Holcomb, M., Rankenburg, K., & Trotter, J. A. (2014). Rapid, high-precision measurements of boron isotopic compositions in marine carbonates. *Rapid Communications in Mass Spectrometry*, 28(24), 2704–2712. <https://doi.org/10.1002/rcm.7065>
- Mehrback, C., Culberson, C., Hawley, J., & Pytkowicx, R. (1973). Measurement of the apparent dissociation constants of carbonic acid in seawater at atmospheric pressure. I. *Limnology & Oceanography*, 18(6), 897–907. <https://doi.org/10.4319/lo.1973.18.6.0897>
- Montagna, P., McCulloch, M., Douville, E., Correa, M. L., Trotter, J., Rodolfo-Metalpa, R., et al. (2014). Li/Mg systematics in scleractinian corals: Calibration of the thermometer. *Geochimica et Cosmochimica Acta*, 132, 288–310. <https://doi.org/10.1016/j.gca.2014.02.005>
- Mucci, A. (1983). The solubility of calcite and aragonite in seawater at various salinities, temperatures, and one atmosphere total pressure. *American Journal of Science*, 283(7), 780–799. <https://doi.org/10.2475/ajs.283.7.780>
- Noireaux, J., Mavromatis, V., Gaillardet, J., Schott, J., Montouillout, V., Louvat, P., et al. (2015). Crystallographic control on the boron isotope paleo-pH proxy. *Earth and Planetary Science Letters*, 430, 398–407. <https://doi.org/10.1016/j.epsl.2015.07.063>
- Otto-Btiesner, B. L., Brady, E. C., Fasullo, J., Jahn, A., Landrum, L., Stevenson, S., et al. (2016). Climate variability and change since 850 CE: An ensemble approach with the Community Earth System Model. *Bulletin of the American Meteorological Society*, 97(5), 735–754. <https://doi.org/10.1175/bams-d-14-00233.1>
- Pelejero, C., Calvo, E., McCulloch, M. T., Marshall, J. F., Gagan, M. K., Lough, J. M., & Opydyke, B. N. (2005). Preindustrial to modern interdecadal variability in coral reef pH. *Science*, 309(5744), 2204–2207. <https://doi.org/10.1126/science.1113692>
- Reed, E. V., Cole, J. E., Lough, J. M., Thompson, D., & Cantin, N. E. (2019). Linking climate variability and growth in coral skeletal records from the Great Barrier Reef. *Coral Reefs*, 38(1), 29–43. <https://doi.org/10.1007/s00338-018-01755-8>
- Reed, E. V., Thompson, D. M., Cole, J. E., Lough, J. M., Cantin, N. E., Cheung, A. H., & Edwards, R. L. (2021). Impacts of coral growth on geochemistry: Lessons from the Galápagos Islands. *Paleoceanography and Paleoclimatology*, 36(4), e2020PA004051. <https://doi.org/10.1029/2020pa004051>
- Reynolds, R. W., Rayner, N. A., Smith, T. M., Stokes, D. C., & Wang, W. (2002). An improved in situ and satellite SST analysis for climate. *Journal of Climate*, 15(13), 1609–1625. [https://doi.org/10.1175/1520-0442\(2002\)015<1609:aias>2.0.co;2](https://doi.org/10.1175/1520-0442(2002)015<1609:aias>2.0.co;2)
- Reynolds, R. W., Smith, T. M., Liu, C., Chelton, D. B., Casey, K. S., & Schlax, M. G. (2007). Daily high-resolution-blended analyses for sea surface temperature. *Journal of Climate*, 20(22), 5473–5496. <https://doi.org/10.1175/2007jcli1824.1>
- Ross, C. L., DeCarlo, T. M., & McCulloch, M. T. (2019). Environmental and physiochemical controls on coral calcification along a latitudinal temperature gradient in Western Australia. *Global Change Biology*, 25(2), 431–447. <https://doi.org/10.1111/gcb.14488>
- Ross, C. L., Falter, J. L., & McCulloch, M. T. (2017). Active modulation of the calcifying fluid carbonate chemistry ( $\delta^{13}\text{C}$ ,  $\text{B}/\text{Ca}$ ) and seasonally invariant coral calcification at sub-tropical limits. *Scientific Reports*, 7(1), 1–11. <https://doi.org/10.1038/s41598-017-14066-9>
- Sayani, H. R., Thompson, D. M., Carilli, J. E., Marchitto, T. M., Chapman, A. U., & Cobb, K. M. (2021). Reproducibility of coral Mn/Ca-based wind reconstructions at Kirimati Island and Butaritari Atoll. *Geochimica, Geophysics, Geosystems*, 22(3), e2020GC009398. <https://doi.org/10.1029/2020gc009398>
- Schoepf, V., D'Olivo, J. P., Rigal, C., Jung, E. M. U., & McCulloch, M. T. (2021). Heat stress differentially impacts key calcification mechanisms in reef-building corals. *Coral Reefs*, 40(2), 459–471. <https://doi.org/10.1007/s00338-020-02038-x>
- Schoepf, V., Grottoli, A. G., Levas, S. J., Aschaffenburg, M. D., Baumann, J. H., Matsui, Y., & Warner, M. E. (2015). Annual coral bleaching and the long-term recovery capacity of coral. *Proceedings of the Royal Society B: Biological Sciences*, 282(1819), 20151887. <https://doi.org/10.1098/rspb.2015.1887>
- Sen, S., Stebbins, J., Hemming, N., & Ghosh, B. (1994). Coordination environments of B impurities in calcite and aragonite polymorphs: A <sup>11</sup>B MAS NMR study. *American Mineralogist*, 79(9–10), 819–825.
- Sevilgen, D. S., Venn, A. A., Hu, M. Y., Tambutte, E., de Beer, D., Planas-Bielsa, V., & Tambutte, S. (2019). Full in vivo characterization of carbonate chemistry at the site of calcification in corals. *Science Advances*, 5(1), eaau7447. <https://doi.org/10.1126/sciadv.aau7447>

- Shen, C.-C., Edwards, R. L., Cheng, H., Dorale, J. A., Thomas, R. B., Moran, S. B., & Edmonds, H. N. (2002). Uranium and thorium isotopic and concentration measurements by magnetic sector inductively coupled plasma mass spectrometry. *Chemical Geology*, 185(3–4), 165–178. [https://doi.org/10.1016/s0009-2541\(01\)00404-1](https://doi.org/10.1016/s0009-2541(01)00404-1)
- Shen, G. T., Cole, J. E., Lea, D. W., Linn, L. J., McConaughey, T. A., & Fairbanks, R. G. (1992). Surface ocean variability at Galapagos from 1936–1982: Calibration of geochemical tracers in corals. *Paleoceanography*, 7(5), 563–588. <https://doi.org/10.1029/92pa01825>
- Spalding, M., Burke, L., Wood, S. A., Ashpole, J., Hutchison, J., & Zu Ermgassen, P. (2017). Mapping the global value and distribution of coral reef tourism. *Marine Policy*, 82, 104–113. <https://doi.org/10.1016/j.marpol.2017.05.014>
- Sutton, A. J., Feely, R. A., Maenner-Jones, S., Musielwicz, S., Osborne, J., Dietrich, C., et al. (2019). *Autonomous seawater pCO<sub>2</sub> and pH time series from 40 surface buoys and the emergence of anthropogenic trends* (1 ed. Vol. 11, pp. 421–439). Earth System Science Data.
- Sutton, A. J., Feely, R. A., Sabine, C. L., McPhaden, M. J., Takahashi, T., Chavez, F. P., et al. (2014). Natural variability and anthropogenic change in equatorial Pacific surface ocean pCO<sub>2</sub> and pH. *Global Biogeochemical Cycles*, 28(2), 131–145. <https://doi.org/10.1002/2013gb004679>
- Swart, P. K. (1983). Carbon and oxygen isotope fractionation in Scleractinian corals: A review. *Earth-Science Reviews*, 19(1), 51–80. [https://doi.org/10.1016/0012-8252\(83\)90076-4](https://doi.org/10.1016/0012-8252(83)90076-4)
- Thompson, D. M. (2021). Environmental records from coral skeletons: A decade of novel insights and innovation. *Wiley Interdisciplinary Reviews: Climate Change*, 13(1), e745. <https://doi.org/10.1002/wcc.745>
- Wall, M., Fietzke, J., Crook, E., & Paytan, A. (2019). Using B isotopes and B/Ca in corals from low saturation springs to constrain calcification mechanisms. *Nature Communications*, 10(1), 1–9. <https://doi.org/10.1038/s41467-019-11519-9>
- Wall, M., Fietzke, J., Schmidt, G. M., Fink, A., Hofmann, L., De Beer, D., & Fabricius, K. (2016). Internal pH regulation facilitates in situ long-term acclimation of massive corals to end-of-century carbon dioxide conditions. *Scientific Reports*, 6, 30688. <https://doi.org/10.1038/srep30688>
- Weber, J. N., & Woodhead, P. M. (1972). Temperature dependence of oxygen-18 concentration in reef coral carbonates. *Journal of Geophysical Research*, 77(3), 463–473. <https://doi.org/10.1029/jc077i003p00463>
- Zeebe, R. E., & Wolf-Gladrow, D. (2001). *CO<sub>2</sub> in seawater: Equilibrium, kinetics, isotopes* (No. 65). Gulf Professional Publishing.